Palacký University Olomouc

Faculty of Science

Department of Geology

Porosity and Pore Pressure Estimation from Well Log Data of Tertiary Khurmala Formation, Kurdistan Region/Iraq

Bachelor thesis

Aran Salar Hamashareef

Petroleum Engineering (B0724A330002)

Fulltime study

Supervisor: Prof. Mgr. Ondrej Babek

Olomouc 2023

Bachelor thesis

Anotace:

Terciérní souvrství Khurmala je tvořeno lagunárními krystalickými vápenci a dolomity s vložkami různých klastických hornin. Cílem této studie je změřit a provést odhad porozity, pórového tlaku a kompartmentalizaci rezervoáru khurmalského souvrství na povrchu, a pod povrchem v ropném poli. Eatonovu metodu lze použít k odhadu pórového tlaku z dat akustické karotáže. Základním předpokladem je vzájemný vztah mezi pozorovanou dobou průchodu (transit time) v karotážních datech a dobou průchodu v normálním trendu kompakce (Normal Compactian Trend, NCT). Objemovou hustotu (bulk density) lze určit z akustické karotáže (sonic log) a porovnat s objemovou hustotou odvozenou z hustotní karotáže (density log) s cílem posoudit zda je možné akustickou karotáž použít jako alternativu k odvození objemové hustoty a ke stanovení litostatického tlaku. Na základě odhadnutého pórového tlaku lze rezervoár rozdělit do tlakových zón. K odhadu porozity a identifikaci litologie se používají hustotní a neutronová karotáž. K ověření karotážení porosity lze použít I výbrusy horniny. Gamakarotáž ukazuje, že obsah jílů (shaliness) v khurmalském souvrství je 20 %, zatímco graf "neutron-density" ukazuje, že rezervoár se skládá převážně z vápence a dolomitického vápence. Model porozity ukázal, že spodní části souvrství vykazuje dobrou pórovitost a dobrou permeabilitu. Odhad pórového tlaku a modelování na základě akustické karotáže ukázaly, že pórový tlak souvrtství se vyskytuje pod 1550 m a normální trend zhutňování se zvyšuje směrem do hloubky souvrství.

Annotation:

The Tertiary Khurmala Formation is a lagoonal crystallized limestone, dolomite with interbeds of different clastic rocks. The aims of this study are to measure and estimate the porosity, estimation of pore pressure, and compartmentalization of the reservoir of the Khurmala Formation in an outcrop and Oil Field. The Eaton method can be used to estimate the pore pressure from sonic log data. The basic assumption is the interrelation between observed transit time from log reading and normal transit time that locates on the normal compaction trend (NCT). The bulk density can be determined from the sonic log and show matching with the bulk density derived from the density log to demonstrate that the sonic log can be used as a good alternative to obtain the bulk density and consequently to determine lithostatic pressure. Based on estimated pore pressure, the reservoir can be divided into pressure zones. Density and neutron logs are used to estimate porosity and lithology identification. The thin sections can also be used to validate pores from log data. The gamma-ray log revealed that the volume of shale in the Khurmala Formation is 20%, and the neutron-density cross-plot showed that the reservoir consists mainly of limestone and dolomitic limestone. The porosity model showed that fair and good porosity and permeability are present in the lower part of the formation. Pore pressure estimation and modeling based on sonic log showed that the formation pore pressure occurs below 1550 m, and the normal compaction trend has increased into the deep of the formation.

I declare that I have prepared the bachelor's thesis myself and that I have stated all the used information resources in the thesis.

In Olomouc, April 26, 2023 …………………………………

Aran Salar Hamashareef

Acknowledgement

Acknowledgements First and foremost, I offer my sincere gratitude to my dearest parents for their undying love, patience, and support, without their encouragement, it would have been impossible for me to continue and finish my studies. I would like to thank my supervisor Prof. Mgr. Ondrej Babek and my Adviser Mr. Hussein. S Hussien, for their willingness to supervise and advising me in my research. their endless support, direction and encouragement have helped me a lot during the writing up of my study. I would like to show my appreciation to all my teachers and classmates at Palacky University and to all who helped me one day to be here, particularly in Petroleum Engineering and Geology Department for their support I get it during the writing up of my research.

Table of Contents

List of Figures

Chapter 1: Introduction

1.1 Preface

The Kirkuk Group, Euphrates Formation, and Jeribe In the Zagros folded zone, the formation was identified as the three main reservoirs in the Tertiary petroleum system in Kurdistan region, Iraq, according to Jassim and Goff (2006). Formations of the Eocene Avanah and Paleocene Sinjar, which comprise the Avanah and Khurmala domes, are among the main reservoir rocks of the Kirkuk oil field (Aqrawi et al., 2010). Additionally, the Chamchamal block, Taq Taq, and Tawke oil fields in Kurdistan's Zagros basin have anisotropic reservoir rock units from the Eocene Pilaspi Formation.By contrast, the Paleocene Khurmala Formation has not been proven as a producer of reservoir rock in newly found oil wells in the Kurdistan Region or previously established fields in Tawke Oil Field. Therefore, in order to understand the reservoir potentiality of this deposit in the tertiary petroleum system, only a very small amount of study on reservoir characterisation for this interval has been undertaken. The Khurmala Formation's petrophysical properties and reservoir quality were assessed in order to determine the logical factors which affected rock retention capacity for hydrocarbons and production efficiency, this study used a set of well log (borehole)data from Tawke oil field.The Khurmala Formation in northern Iraq has been studied for a long time. Bellen, 1953 recognized the Khurmala Formation for the first time in well K-114 at Kirkuk. The formation contains oolitic dolomite and crystalline limestone that interfinger with sandstone beds (from the previous Kolosh Formation) that contain clasts of chert, flint, radiolarite, and greenstones of silt and sand size. Anhydrite (perhaps secondary) is also occasionally found (Bellen et al., 1959).

1.2 Geological setting

The Arabian and Eurasian plates collided in the Late Cretaceous to early Miocene, producing a Zagros mountain range. Iran's plateau and the Zagros Mountains both gain height annually as a result of this process, which is still active today at a rate of around 25 mm. In the southeast of Iran, the Zagros Mountains are a strip of deformed crustal rocks. From eastern Turkey in the northwest through the Gulf of Oman in the southeast, they span a distance of more than 1500 kilometres. From northeast to southwest, Alavi (2004) The Zagros orogens were divided into three tectonic groups: the UrumiehDokhtar magmatic assemblage, and the Sanandaj-Sirjan zone (the Zagros imbricate zone), and the Zagros Fold-Thrust belt (Fig.1). This belt's in the deformation intensity is increasing in the northeast. (Alavi 1994). The three main tectonic zones identified by Jassim and Goff in Iraq in 2006 in the Zagros orogenic belt are the stable shelf, the unstable shelf, and the susture zone. Mesozoic and Cenozoic periods yield short-wavelength, high-amplitude folds with south-to-southwest vergences in the high-folded zone (Fouad, 2014). The deformation style of fault-related folds is halfway between fault-bend folds and fault propagation folds (Zebari, 2013). As one proceeds north and northeast, the amount of shortening and the intensity of deformation increase (Fouad 2014). In the northern region of Iraqi territory, the Zagros-Taurus Fold and Thrust belt contains the Tawke anticlinal structure. This structure is situated in the tectonic transition zone between the Low Folded Zone to the south and the Imbricated Zone to the north in Iraq. It was clear that the area's topography was reflecting structural elements. Folds, faults, and large cracks have a crucial role in forming or adding complexity to the region.The Tawke Oil field is located within the Tawke anticlinal structure in the city of Zakho-Duhok governorate, northern Iraq, and is elevated 500 m above sea level. Tawke oil field location is in the Zagros-Taurus Folds and reach belt's in High Folded Zone. It is one of Iraq's greatest oil fields, producing high-gravity oil from a fractured reservoir at a depth of less than one kilometer. DNO, the Norwegian oil and Gas Company, redeveloped the field beginning in 2004 and began production in June 2007. Early in 2009, the Tawke export infrastructure was linked to the Iraq-Turkey pipeline system to provide crude oil to the international market (Mzuri and Omar, 2016).
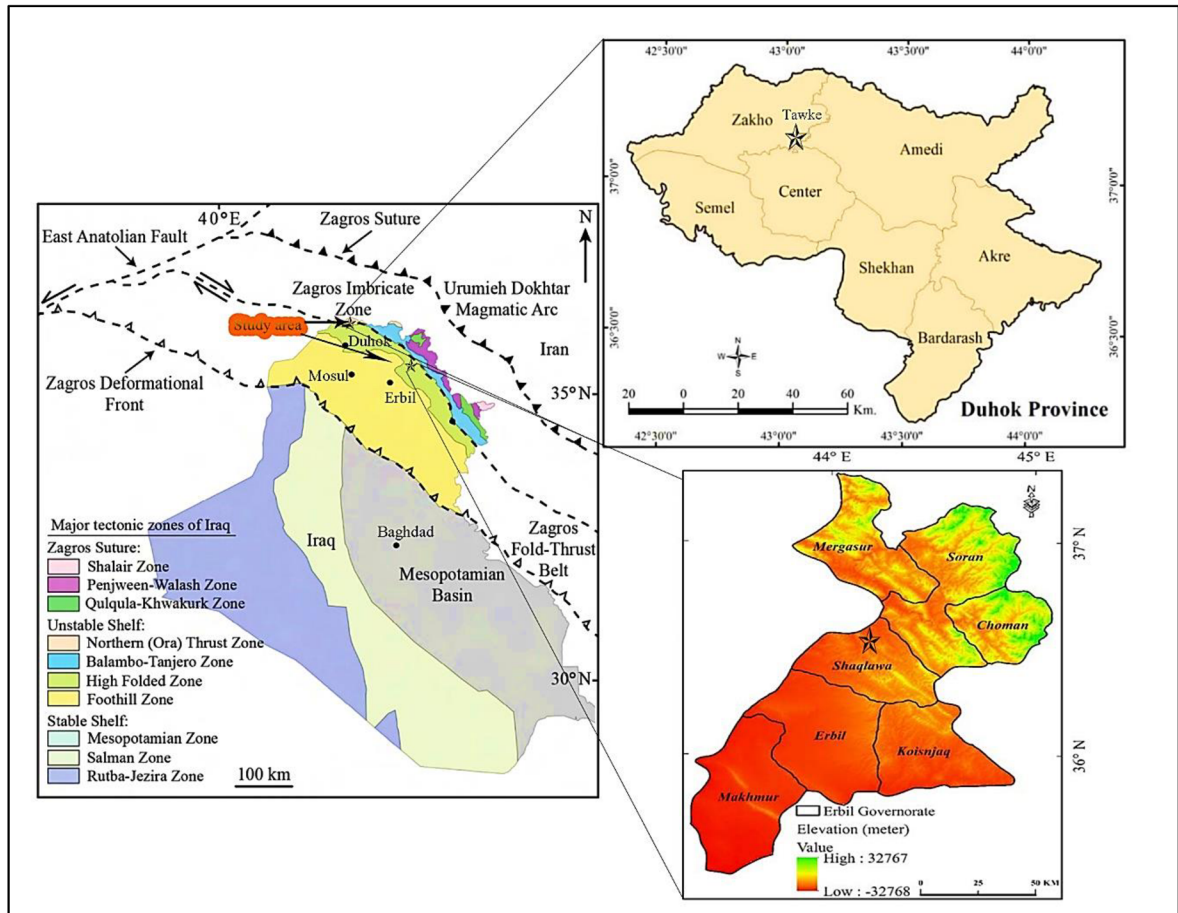
Figure 1 the studied area in the tectonic Iraqi map (Doski 2019)

1.3 Aims of the study

The main aims of this study are:

1-Petrographic study to identify porosity of the Khurmala Formation in the studied area.

2-Determination of petrophysical properties such as porosity, shale content, water, and hydrocarbon saturation based on set of wireline log data.

3-Estimation of pore pressure and compartmentalization of the reservoir, using core sample data.

Chapter 2: literature Review

The Middle East is home to nearly 15% of the world's oil reserves, in which the carbonate rock type is predominant in producing reservoirs. (Hollis, 2011; Hollis et al., 2017; Jafarian et al., 2017; Adam et al., 2018). In Iraq, the Zagros basin is characterised by an extension of oil systems and a heterogeneous distribution of reservoir types, such as Triassic. (Ryder Scott, 2011), Jurassic (Sherwani and Zangana, 2017), Cretaceous (Al-Qayim and Rashid, 2012; Rashid et al, 2017; Ghafur and Hasan, 2017) and Tertiary reservoir rocks (Al-Qayim and Othman, 2012; and Hussein et al., 2018). The Khurmala Formation sediments are found in various locations throughout north Iraq as tongues within the upper part of the Kolosh Formation (Early Eocene age, Alveolina primaeva and Saudia labyrinthica appear to be restricted to the Late Palaeocene; Daviesina, Dictyokathina simplex, Idalina sinjarica, Miscellanea miscella, Nummulites fraasi and Operculina salsa to the Late Palaeocene-Early Eocene; and Alveolina oblonga and Assilina placentula to the Early-Mid Eocene.). The formation is 185 meters thick in the type area, 173 meters thick in Kirkuk 117, 115 meters thick in Taq Taq-l, and 262 meters thick in Atshan1. Because of the presence of sediments from the underlying series, the measured thickness in well Jabal Kand-l of 606 m is probably too high. Al-Banna et al. (2006) studied Formation of khurmala in the Bekhair anticline and showed a bundle of both clastic sediments and carbonate, measuring about 60 meters thick and dating to the Early Eocene, makes up the examined surface part of the Khurmala Formation, which is located northeast of Duhok city in northern Iraq. The clastic material contained two lithofacies associated with the depositional environment of estuaries, however the carbonate sediment is composed of four microfacies associations given to sholagoon (Kh1), intertidal (Kh1, Kh3), al bank (Kh2), and supratidal (Kh4). The Khurmala Formation was given a depositional model. Microfacies exhibit diagenetic dissolution and dolomitization processes (Kh3) (fig. 2).

Age	Stable Platform		Unstable Platform			Imbricate Zone
	Rutba - Jazira Z.	Salman Z.	Mesopotamian Zone	Foot Hill Zone	High Folded Z.	
Eocene	Rus	Rus	Aaliji	Sinjar	Khurmala	Suwais Red Beds
Paleocene	Akashat / Umm er Radhuma	Umm er Radhuma			Kolosh	
Maastrichtian	Jeed / Digma / Tayarat / Semhat		Hartha	Shiranish	Aqra-Bekhme	Tanjero
Campanian			Sa'di			
Santonian			Tanuma	Kometan		
Coniacian			Khasib			
Turonian	Mishrif	Kill		Mishrif	Gulneri	Upper Balambo
Cenomanian	Rutba	Ahmadi	Rumaila		Dokan	

Figure 2 Chronostratigraphy chart of tertary and cretaceous sections in Iraq after Van Bellen et al., 1959, Buday, 1980, Jassim and Goff, 2006

Al-Lihaibi (2012) studied Khurmala Formation in Dokan area and he claimed within the Khurmala limestone Formation in the Dokan region of northeastern Iraq, diagenesis was investigated. The study identified several diagnostic mechanisms. at the limestones were influenced by a series of processes including micrazole envelope, dolomitization, dissolution, neomorphology, cementation and mechanical and chemical compaction. The investigation identified four diagnostic zones. They are mixing zone, the burial zone (mechanical and chemical compaction), meteoric phreatic zone (dissolution, neomorphism, cementation), and marine zone (micrite envelope). The study found that periodic changes in sea level have had an impact on diagenetic processes and their paragenetic sequence, according to the history of diagenesis and their sequence.Assad and Balaky (2018). In the Zenta area of the Aqra district in northern Iraq's Kurdistan region, the microfacies and environmental studies of the Khurmala Formation were studied. The formation is composed of medium to thick bedded yellow limestone that is interbedded with thin layers of marl and mudstone, as well as bedded grey dolomitic limestone that is primarily bituminous with chert nodules. Three significant microfacies, as well as two different lithological units, were found in the limestones of the investigated region based on field evidence and petrographic study. dolomitic limestone unit with thick bedding and the marl limestone unit with bedding.

Petrographic data, facies, and textural studies suggest that the shelf lagoon setting of a shallow marine environment is where the Khurmala Formation was deposited.Rashid et al., (2020) studied the Formation of khurmala in the Taq oil field utilizing wireline log analysis, drilling cuttings, and fluid distribution to better understand Reservoir potentiality and dispersion of fluids. The formation consisted of dolostone and Dolomitic limestone, with clay layers intercalating among the known strata. The computed volume of shale contains a high content of clay with certain spots in the gamma ray showing an entire amount of shale. The formation consisted of dolostone and Dolomitic limestone, with clay layers intercalating among the known strata. The clay content is very high in the computed volume of shales, with some gamma ray sites containing 100% shale. The Authors divided classified the Formation of Khurmala into five units of porosity which is based on the corrected log-derived bulk porosity (Kh-1 to 5). The first (Kh-1), third (Kh-3), and fifth (Kh-5) porosity units had a normal porosity of more than 10%, which is regarded an excellent reservoir unit in terms of porosity, however the shale component of these units affected the reservoir quality.Al-Qayim and Barzani (2021) They studied the facies and strata of the Khurmala formation in the Duhok area, based on field observations and microscopic studies, and the types of facies of the formation have been identified. The types of facies of the formation have been identified. It appears that the Khurmala Formation is deposited in a shallow shelf area of supratidal, intertidal, and partially restricted lagoonal facies with a silicic-dominated coastal plain in Spindar and Birkyat. The Khurmala Formation in Spindar and Birkyat seems to be deposited in a shallow shelf setting of supratidal, intertidal, and semi-restricted lagoonal facies with siliciclastic-dominated coastal plain.Assad et al. (2022) studied the depositional environment of the Khurmala Formation (Paleocene-Eocene) in Iraq's High Folded Zone has been examined in the Nerwa section, the southern limb of the Berat anticline. studied the depositional environment of the Khurmala Formation (Paleocene-Eocene) in Iraq's High Folded Zone has been examined in the Nerwa section, the southern limb of the Berat anticline. The formation consists of three parts; fossiliferous bedded limestone, major dolomitic limestone and bedded marly dialastic limestone. Five main microfacies were identified from a petrographic study of carbonate rock: lime mud, lime wackestone, lime packstone, grainstone and boundstone; one lithoformic conglomerate. Two facies associations which indicate deposition in lagoonal environment, including reefs have been established by microfacies and field characteristics of the formation

Chapter 3: Material and methods

3.1 Technical methods and material

The porosity and permeability are calculated by using log data tawke-1 field in Kurdistan region of Iraq. The environmental adjustments and reservoir parameters like porosity, relative permeability, water, and hydrocarbon saturation (fluid content) were computed using a software tool. The digitized LAS files (LAS files, short for Log ASCII Standard files, are digital files used to store and transmit well log data in the oil and gas industry. They contain well log data that is typically recorded by wireline tools during drilling operations), which comprise calliper gamma ray, density, neutron, acoustic, and resistivity records, are loaded into the Interactive Petrophysics program (IP-V 4.4) which is a software application used for analysing and interpreting geological data in the petroleum industry. The reading measurements are obtained as one reading per 0.2 meters. The log curves are evaluated for depth with each other. The depth-matched log curves were then compared to the available gamma ray data, which was used as a reference material for an evaluation of depth.

On the other hand, the pore pressure models allow you to evaluate the subsurface pressure encountered within a well, then enable you to model the overburden pressure, and pore pressure within the lithology. rock physics modules can be found under advanced interpretation- rock physics.

The first step of the module is to perform a density estimation calculation based on the sonic curve within the data set. In this section develop density curves using the P-wave (Vp) velocity and imperial relationships. The lithology used is either gardener, Bellotti, or Lindseth. Here we generate an output set so the curves made can be easily identified later. Select run to perform calculations, this will then generate the curves.

The next step is to perform an overburden gradient calculation, for overburden gradient calculations a depth curve is required, additionally, Kelly bush (KB) height or water depth

7

and water density require to be used, now select the density curves previously made for the gardener, Bellotti or Lindseth. Next, name your output curve set as required. In this study, a new curve set has been made so the curves will be easy to identify. Select Ok to perform the calculation. As you see two new curves have been added to the well. Then press make plot to examine the results.

The final step now is to run both of pore and fracture pressure gradient calculations. Input the well data. Select the previously made overburden gradient, select depth curve and the shale discriminator curve. The Kelly bushing height, water depth and water density will be automatically filled from the well header information here we must choose appropriate units

The next stage is determining what the pore pressure gradient and pressure will be calculated from, here using sonic curve. Next select the method for calculating fracture gradient and pressure, either select from Eaton, Mathew or baker or wood.

In this study, the Eaton method will be used, select the output curve again that will be computed after the analysis has run then select pore pressure tolerance percentage

In the general tab you can set the depth interval over which the analysis is performed the shale cut-off and the hydrostatic gradient and the hydrostatic gradient units.

The next stage is inputting the well data. The first sub tab is the casing string, input information leak off test pressure. And the compute mud weight.

The final tab is the results cross plot tab, choose to display the plotted model as depth vs. pressure or depth vs. pressure gradient .

Final press Ok and see the results, the pore pressure is calculated in shale intervals.

The vertical line of the shale discriminator track is the shale cut-off,

3.2 Thin section analysis

A thin section is a thin part of rock which is 30 microns thick which glued in the glass slide. First operation is to cut rocks by rock saw machine (Fig.3) for suitable size for polishing and gluing it to the glass (Fig.4) the next step is in thin section process is grinding and polishing the rock sample to be epoxide to the glass on the glass plate and powdered grits .Then grinding of one side of the glass and then gluing the rock samples to the glass and cutting the remaining rock after gluing the glass to the rock sample the thin section will be done and it will need grinding the thin section on the glass plate and by powdered grits (Fig.5) after a having a smooth side in the thin section it will need the polishing by a machine (Fig.6).

Measuring porosity in the thin sections measured by a program which is called (ImageJ) In petroleum engineering, (ImageJ) can be used to analyze digital images of thin sections to extract important properties such as pore size distribution. This information can then be used to understand the petrophysical properties of the rocks, such as porosity, which are critical in reservoir characterization and modeling.

Thin sections which are used in this project is taken from seven samples in different layers from Shaqlawa out crop in Kurdistan Region of Iraq (Fig. 7)

Figure 3 Rock cutting machine at the Palacky University lab

Figure 4 rock sample with polished and grinded with glass plate and powder

Figure 5 thin section sample grinded with glass plate and powder

Figure 6 thin section polishing machine

3.3 Core sample process

Core plugging apparatus used to make core plugs from rock samples taken from carbonate outcrops. The plugs were ready for the core flooding experiments. This equipment allows core plugs with diameters of 1 to 1.5 in and lengths of 3.5 to 3.5 in. after this the Core cutter apparatus by altering the plug dimensions, the core cutter device was used to change the shape of the created core samples. A cutter machine is used to cut the modification surface and flatten the core surface. The cutter machine was used to produce thin sections for wettability testing in addition to cutting the core. Extraction using the Soxhlet method the pores within the core contain a variety of fluids that must be cleaned before the core flooding test can be done. before core flooding the core, plugs were cleaned with a soxhlet extraction. A heater, solvent cup, sample chamber, condenser, and cooling pump are all part of the soxhlet apparatus. The core plugs were dried in an oven after being cleaned. The oven used in this study was built by the Day Tajhis Aryan Paya (D.T.A.P) Company and can attain temperatures of up to 200 degrees Celsius. porosity meter was used to assess the porosity of the cores. This device evaluates porosity by injecting helium gas into the core sample, which is based on Boyle's and Charles' Law. A gas permeameter was used to determine the permeability of the core plug samples. The apparatus was built to measure permeability while taking into consideration the slip factor and Solution permeability at varied flowrates, back pressures, and injection pressures. A differential pressure transmitter was used to track the differential pressure on both sides of the core sample, and a precision mass flow meter was used to estimate the gas flow rate through the sample

Four samples used for porosity and permeability measuring which they are from Shaqlawa out crop in Kurdistan Region of Iraq (fig.7)

Figure 7 Shaqlawa out-crop in Kurdistan region of Iraq

Chapter 4: Determination of petrophysical properties

4.1. Lithology and mineralogy

A wireline log was used to integrate the lithological description, and a sonic-neutron log cross-plot was used to identify the lithology (Rider and Kennedy, 2011; Krygowski, 2003; Schlumberger, 1997 The overlapping and crossing of neutron density and neutron-sonic logs is the most popular combination method for determining lithology. In addition, a cross-plot between neutrons and sonic logs shows an important conclusion regarding continuous lithological fluctuations at recorded intervals. By using this procedure, you may obtain a single rock type or a combination of two different rock types, such as limestone, dolostone, or dolomitic limestone. Based on the mentioned cross-plot the Khurmala Formation in Tawke-1 consists mainly of limestone and dolomitic limestone (Fig.8) showed that the most plotted points are located on the limestone line where the porosity between 10-15% while the other points have high porosity located between limestone and dolomite lines or as can say dolomitic limestone
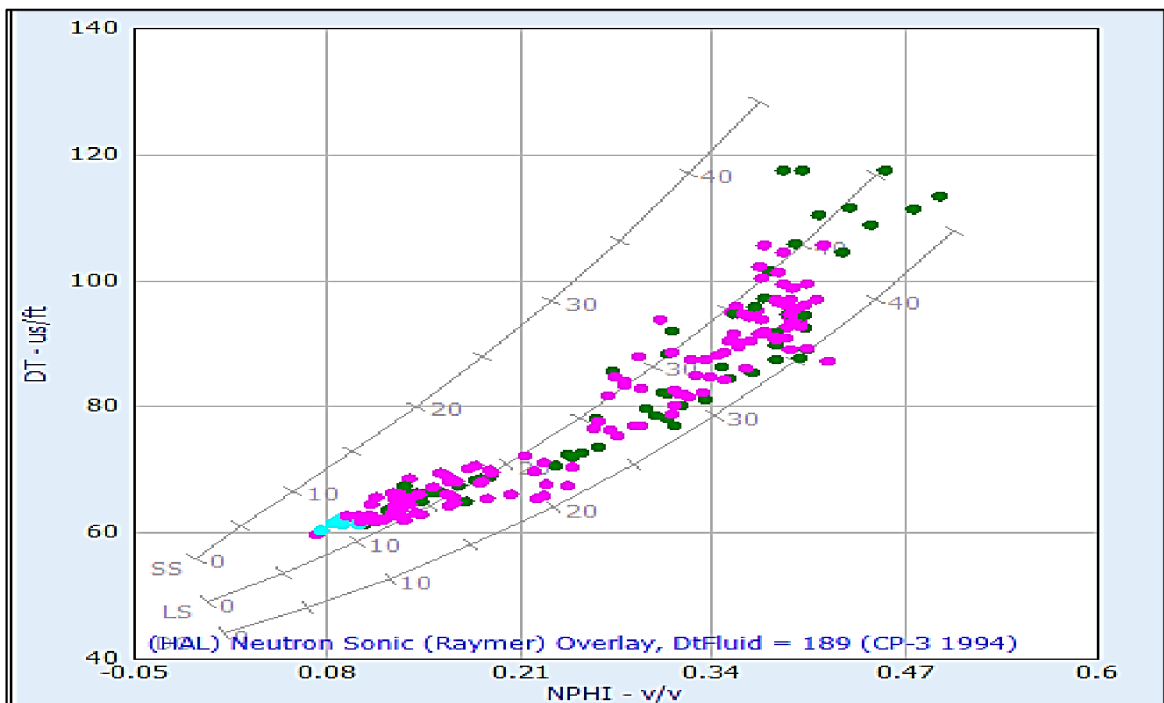
Figure 8 relationship between DT and NPHI shows the lithology of Khurmala Fm.

Determining the lithology and mineralogy of this formation can also be done by using a M-N cross-plots. When the lithology of a formation is more complicated, this approach is applied. This cross-plot requires the acoustic log in addition to the neutron and density logs. The sonic log is a porosity log which quantifies the transit time between intervals (Asquith and Gibson, 1982). Calcite and dolomite are the primary constituents of the Khurmala Formation, according to the M-N cross-plot with some shale that has been observed (Fig. 9).

Figure 9 M-N relationship showing that the selected formation (Khurmala Formation) consists of limestone and dolomite with some points scattered to shale region and secondary porosity (Asquith and Krygowski 2004)

4.2. Shale Volume

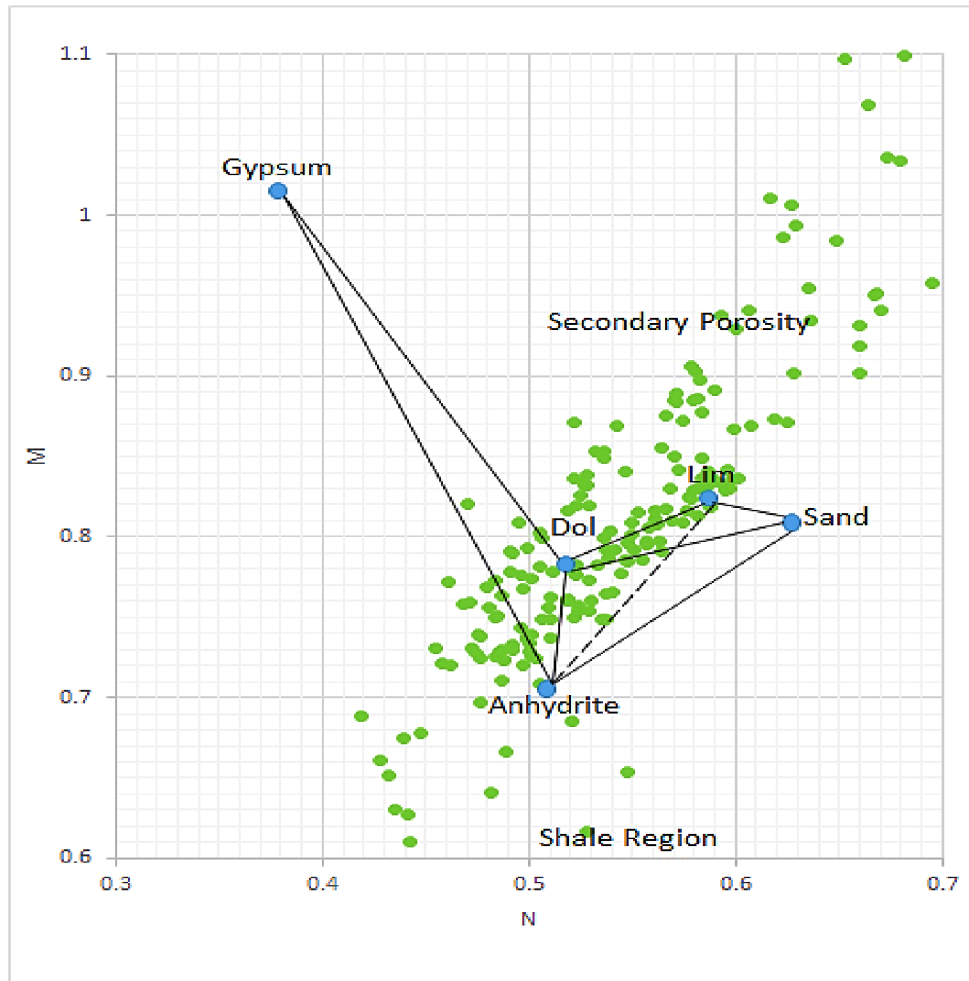The shale of a volume (clay) in a certain interval can be calculated using gamma ray log. Shale volume is the predicted volume, which is often represented in a decimal fraction or percentage (Vsh). Because organic matter may concentrate uranium, its presence in carbonate rocks may have an impact on how much shale is present. Calculating the volume of shale in this first step (Equi.1) is for calculating the gamma ray index (I_{GR}), using the shale baseline (gamma reading = 100 API), clean sand line (gamma reading = 0.0 API), and the gamma ray log measurement from the chosen interval (Bhuyan and Passey, 1994). The best equation is then used to convert the computed gamma ray index (IGR) to shale volume. The Larionov (1969) equation for estimating the amount of shale in Tertiary (young) rocks was employed in this investigation (Equi. 2).

$$IGR = \frac{GR\,log - GRmin}{GR\,max - GRmin} \quad \text{......................} \quad (1)$$

$$Vsh = 0.33(2^{2*GRI} - 1) \text{.................} \quad (2)$$

I*GR*: - Gamma ray index

GR*log:* - Gamma ray reading from log, API

GR*min:* - Minimum gamma ray reading (clean sand or carbonate), API

V*sh:* - Shale volume.

GR*max:* - Maximum gamma ray reading (shale), API

The Khurmala Formation has a maximum gamma ratio of 62 and a lowest gamma reading of 23, as seen in (fig 10). The formation has an average clay concentration of 20%, showing that the chosen formation normally includes more clay, which has an impact on reservoir attributes since a lower shale content often displays clean zone while an increase in shale volume reduces the capacity of an effective reservoir.

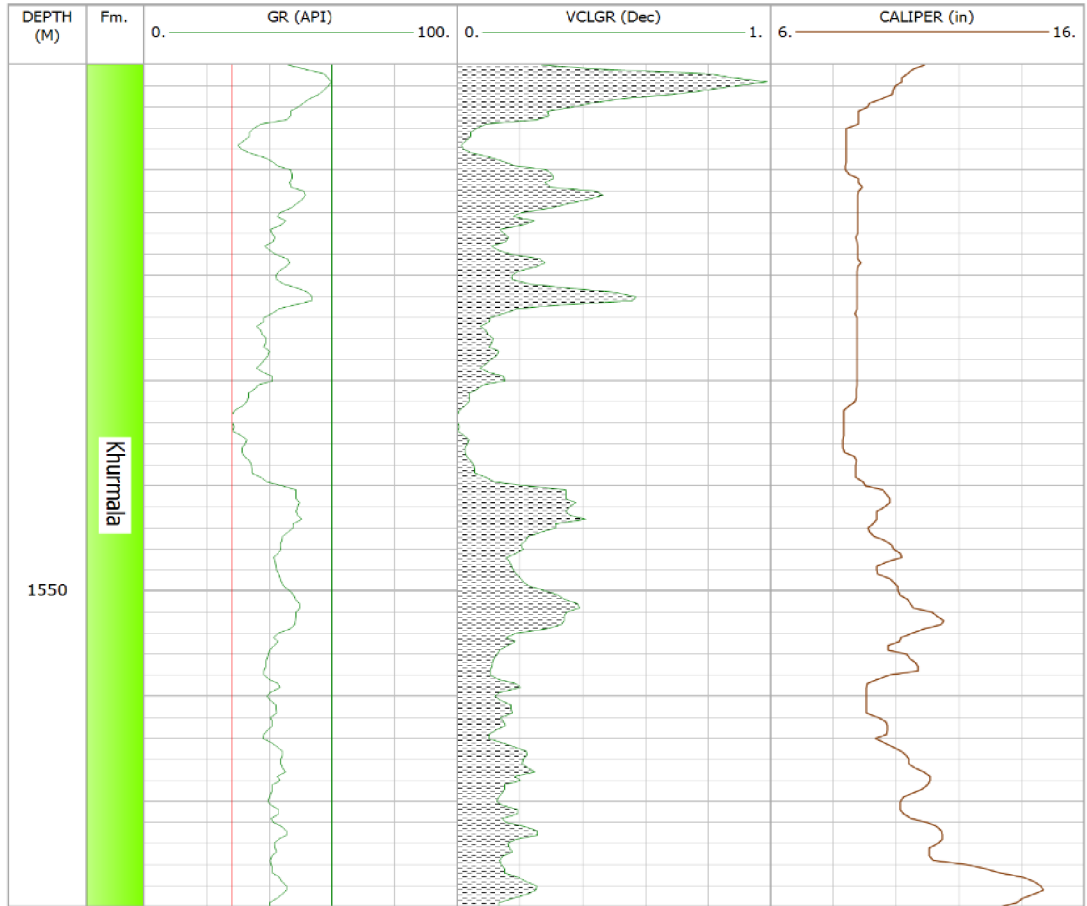In (fig.10) the bit size is equal to 8.5 inches.

Figure 10 Calculated the Shale volume in the Khurmala Formation from (Tawke-1) well

4.3. Water resistivity (Rw)

Pickett's cross-plot, which represented Archie's thought in the form of a visual representation, had its inception in 1966. By plotting the true resistivity (Rt) on the horizontal axis and the effective porosity (φe) then the vertical axis using logarithmic scales for both axes, the parallel lines that represent the water saturation (Sw) may be created. You may read the whole Sw of any plotted point. This approach is based on the idea that porosity, water saturation, and cementation factor (m) all affect real resistivity. The line at complete saturation with water represents the wet resistivity (Ro). On the real resistivity scale, when porosity equals one and the line with a slope of (-1/m) intercepts the vertical scale, water resistivity may be read. The formation water resistivity in the selected interval is too low (0.063) which indicate that the formation water saturation and water-cut not reached to 20% and water free hydrocarbon can be produced in the selected formation, in addition to, this relationship has also been used to calculate the values of the a, n, and m parameters that can be seen on the (Fig.11).
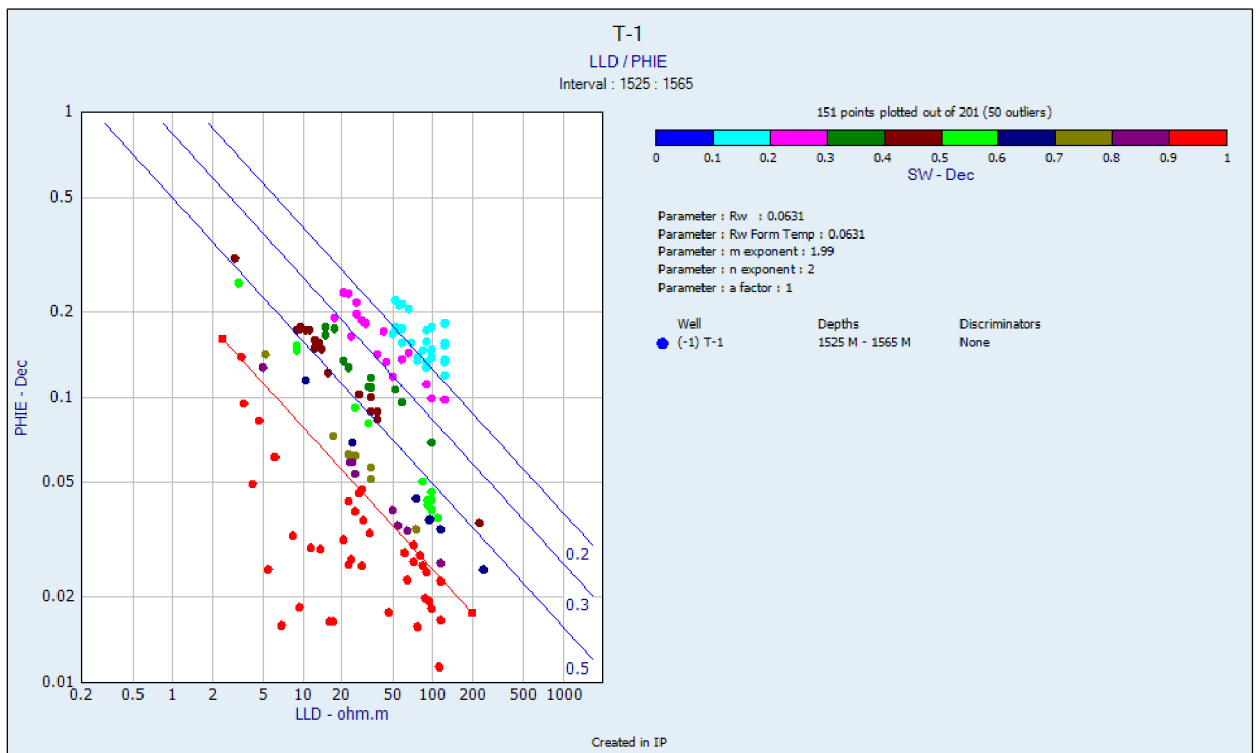
Figure 11 True resistivity vs. effective porosity showing Rw value of the Khurmala Formation in Tawke oilfield

4.4. Buckles model

The determination of the total volume of water shall be carried out using a cross plot of porosity and saturation. Since the amount of water produced by a well may have an effect on the economy, it is essential to comprehend the total water volume and the irreducible saturation of water (Swirr) (Asquith and Krygowski 2004). As can be seen, the Khurmala structure is equally dispersed around the hyperbolic line 0.02 and 0.04 (Fig. 12), implying that the reservoir is homogenous and irreducibly saturated with water. When the volume of bulk water follows hyperbolic lines and is nearly constant, the composition is homogenous and at irreducible water saturation.

Figure 12 Buckle model showing the points of the studied formations on 0.02 hyperbolic and is at irreducible water saturation

4.5 Porosity

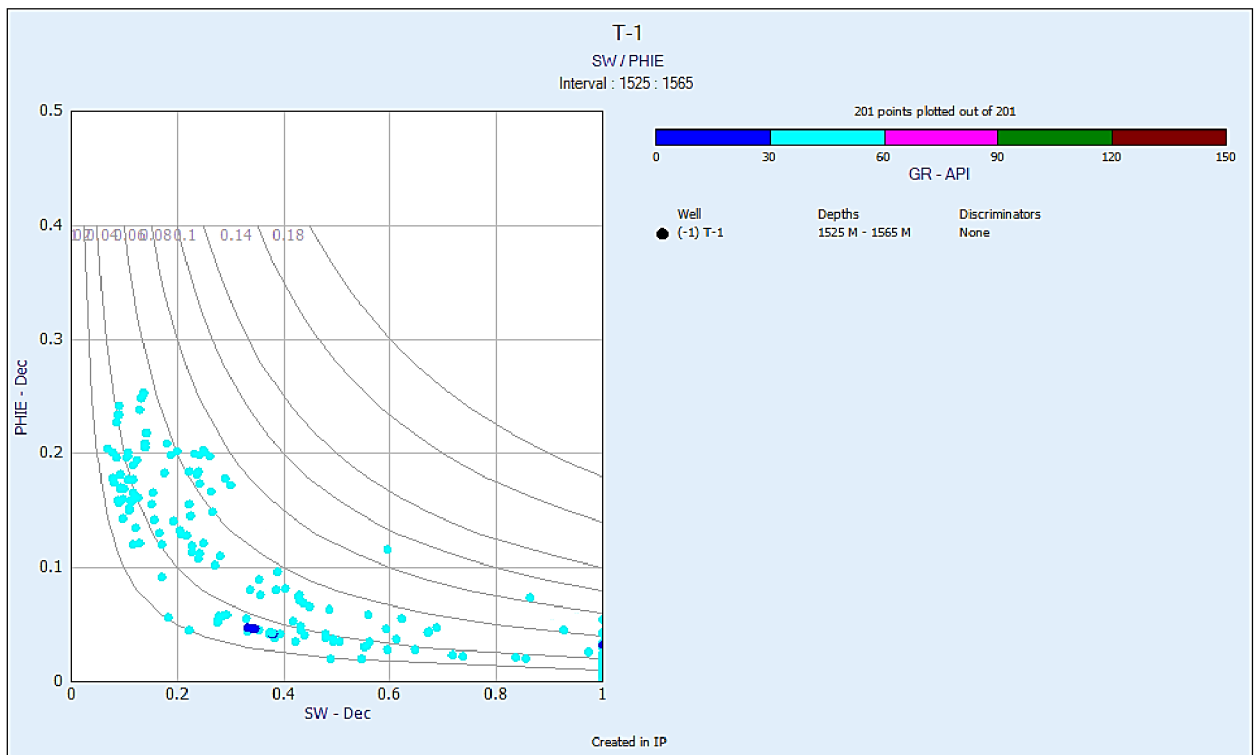Porosity logs—also known as sonic, neutron and density logs—are extensively used to measure porosity in formation evaluation and reservoir quality assessment. Wiley time average (Equi.3) (Wiley and Pachett, 1990; Asquith and Krygowski, 2004) must be used to calculate porosity from the sonic logs and the apparent of density of the fluids inhabiting the pores using the matrix's values (Equi. 4). Additionally, when reading the recorded period, the hydrogen concentration was instantly

$$\boldsymbol{\Phi}S = \frac{\Delta tlog - \Delta tma}{\Delta tfl - \Delta tma} \ \dots \dots \ (3)$$

ϕs: Sonic porosity, fraction

$\Delta t \ log$: Sonic log reading, μs/m

$\Delta t \ ma$: Transit time of matrix, μs/m

$\Delta t \ fl$: Transit time of the mud filtrate, μs/m.

$$\Phi \ \rho \ = \frac{\rho ma - \rho b}{\rho ma - \rho f} \dots \dots \ (4)$$

$\Phi \rho$: Density porosity, fraction

ρma: Matrix density, g/cm^3

$\rho bulk$: Log reading density, g/cm^3

ρfl: Fluid density, g/cm^3.

ΦN= neutron log index

If the formation contains non-gas fluid the formula is

$\Phi t = \Phi D + \Phi N / 2$ ……………… (5)

If the formation contains gas fluid the formula is

$$\sqrt{\frac{\Phi D2 + \Phi N2}{2}} \ \dots \dots \dots \dots \dots \ (6)$$

Effective porosity equation

$$\text{\O}e = \text{\O}t * (1 - \text{Vsh})\dots\dots\dots\dots (7)$$

Nuclear measurements are used in both the density and neutrons and the sonic tool is used to assess the sound (acoustic) properties of the rock. The accuracy of the computed porosity by wireline log is achieved when measuring reservoir properties with a combination of three Porosity Logs. The estimated porosity in this study was obtained using porosity logs adjusted for shale content.

Carbonates lose porosity owing to a combination of pressure dissolution, compaction, and cementation (Mukherjee and Kumar 2018). Because the shale proportion in the Khurmala Formation fluctuates between 19% and 20%, there is a discernible variation between effective and total porosity., The investigated period is divided into two zones (1, 2), both of which are 20m thick (Fig. 12).

4.6. Permeability (K)
4.6.1 Determine permeability from well log

Permeability is the second most important characteristic of a reservoir; the pores must be connected to allow hydrocarbons to flow in and out the reservoir. Permeability, as it refers to the ability of the liquid to move through the rock and is a major regulating factor for information productivity, is one of the most important variables in a reservoir. (Selley, 1985). Minor spacing between rock grains is likely in spongy rock; these spaces will hold liquid, which can occasionally be water, oil, or gas. The permeability of the rock measures how easily this liquid may pass through it.

The precise prediction of permeability in complicated in the carbonate reservoirs is one of the most exciting positions of well log analysis. Using well log data, numerous theories estimate permeability. A few relationships, based on known physical properties or empirically derived relationships, have been developed over time to calculate permeability. Though, none of the existing well logging approaches can quantify it publicly. The Timur mode was employed to estimate formation permeability in the current investigation. Porosity is the most obvious determinant of permeability. This is because larger porosities indicate more and wider fluid flow channels. Different models may be used to predict permeability:

$$K = a * \frac{\text{\O}^b}{Swir^c}\dots\dots\dots\dots\dots (8)$$

For models Timur, Morris Biggs and Schlumberger the following constants are provided: a, b, and c

Morris-Biggs for gas: a= 6241; b = 6 and c = 2

Morris-Biggs for oil: a= 62500; b = 6 and c = 2

Timur: a = 8581; b = 4.4 and c = 2

Schlumberger: a = 10000; b = 4.5 and c = 2
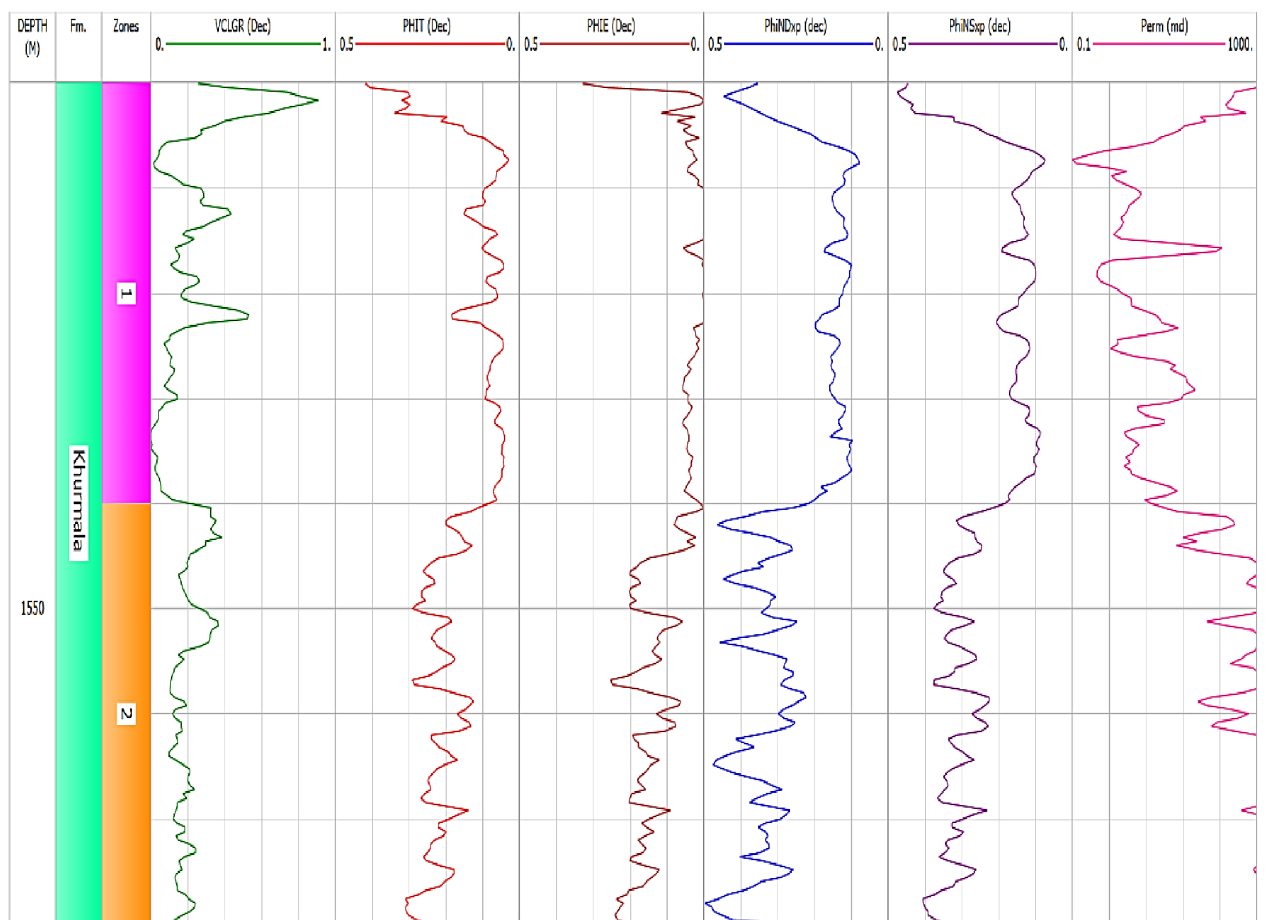
Abbreviations: Vcl GR: clay volume gamma ray; PHIT: Total porosity; PHIE: effective porosity; PhiND: neutron-density porosity; PhiNS: neutron-sonic porosity; Perm: Permeability.

Figure 13 Showing porosities, permeability, and shale volume determination in the selected formatio

24

4.6.2 Permeability Determination from outcrop

Flows fluid with known viscosity through predetermined sample that has known dimensions on a predefined basis and measures pressure drop across the core sample taken in outcrop section, either by setting the fluid to flow at a predetermined pressure difference, or by measuring the rate of flow produced, permeability is measured on cores and samples taken from outcrop in the laboratory. We now need to draw a difference between the utilization of liquids and gaseous fluids. Liquids present a comparatively simple measuring problem since surface geological conditions nearly usually satisfy the requirements for laminar flow and incompressibility of the fluid. There are two issues with using gas as the fluid, which is a practice that is popular in the sector: As a compressible fluid, when measured in volumes per second at the input high pressure end of the sample than at the outlet low pressure end, the gas will move more slowly than at the outlet high pressure end of the sample, where it expands, even though it is moving through the core at the same mass per unit time. To account for the gas compression, the equation that was used to determine the permeability value from the observed values must be changed. Very few gas molecules may fill some of the smaller holes at low gas pressures. If this occurs, the rules we are applying fail, and their application results in an overestimation of permeability. Gas slippage or the Klinkenberg Effect is what causes this. As pressure is raised, the issue is less since there are more gas molecules per volume and the gas is compressed, and it does not exist with liquids because they are considerably denser than gases. By measuring the apparent permeability of gas at various pressure differentials and creating a graphical recording of the observed the permeability versus the mean pressure in the rock samples, gas slippage is adjusted for. The permeability is depicted as a function of $1/Pm = 2/ (P_{in} + P_{out})$ If the pressure in the input gas is Pi and the output pressure is Po, as shown in (Fig.14) Now, a straight line connecting the points should cross the y-axis at $1/Pm = 0$. This quantity, known as the Klinkenberg permeability, really denotes the permeability at which a nearly perfect gas, under infinite pressure, transforms into a nearly perfect liquid. When measuring permeability using gas as the flowing fluid, Klinkenberg (1941) found that the findings were different from those obtained when measuring permeability with a liquid. When flowing gas is used to assess the permeability of a core sample, the result is always larger than when flowing liquid is used. This method is used for the outcrop samples that were obtained in the Khurmala Formation in Shaqlawa section, specifically the sample S3 & S11, where Klinkenberg discovered that for a given porous medium, as the mean pressure increased, the predicted permeability

dropped. In contrast, in the other samples (S4 & S9) the permeability increases with increasing mean pressure (Pm)
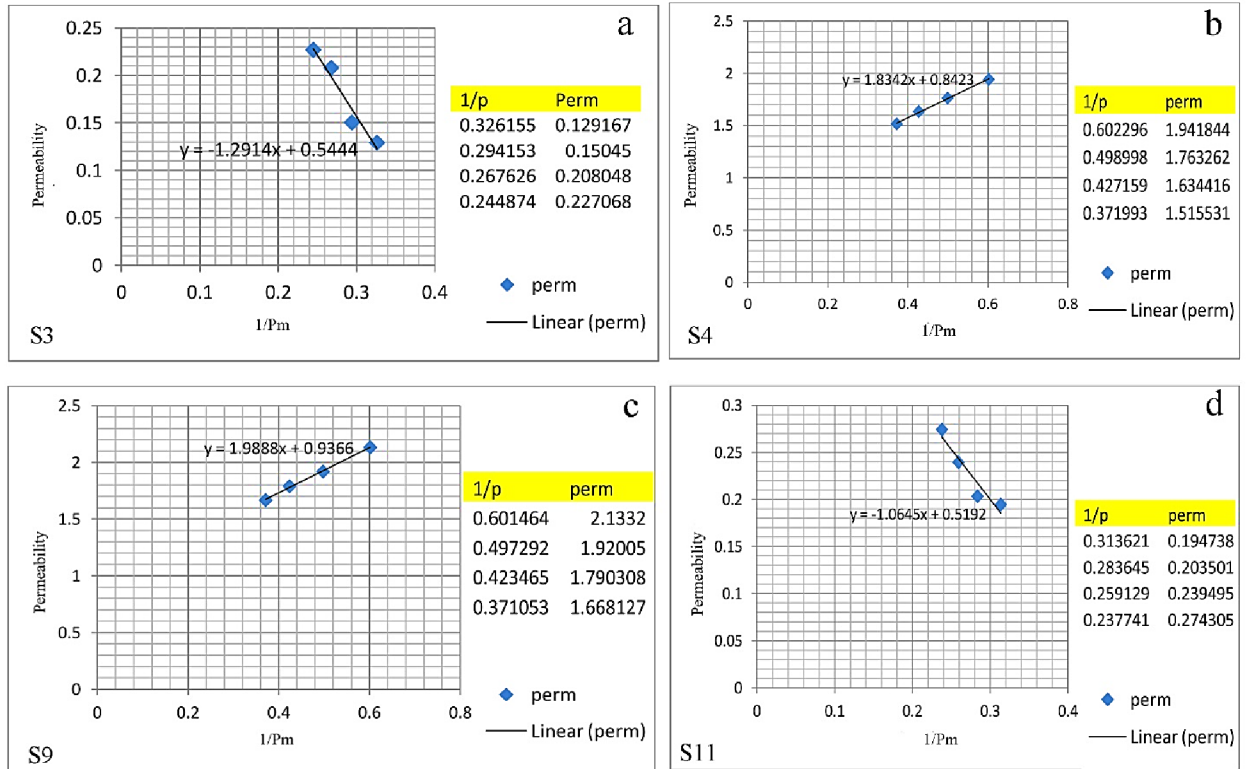
.

Figure 14 Relationship between Pressure mean and permeability for the analysed samples in outcrop section

4.6.3 Relationship between porosity and permeability

Four core samples were taken in Shaqlawa area (outcrop section) to determine porosity and permeability of the Khurmala Formation. There are several ways to evaluate porosity. One is by thin sections, which offers apparent porosity, and another is through helium porosimeter study on core plugs, which yields effective porosity. (Fig 15) also depicts the link between porosity and permeability. The increase in porosity increases permeability because as the number of pores grows, so does interconnectivity, and as a result, permeability rises as well.
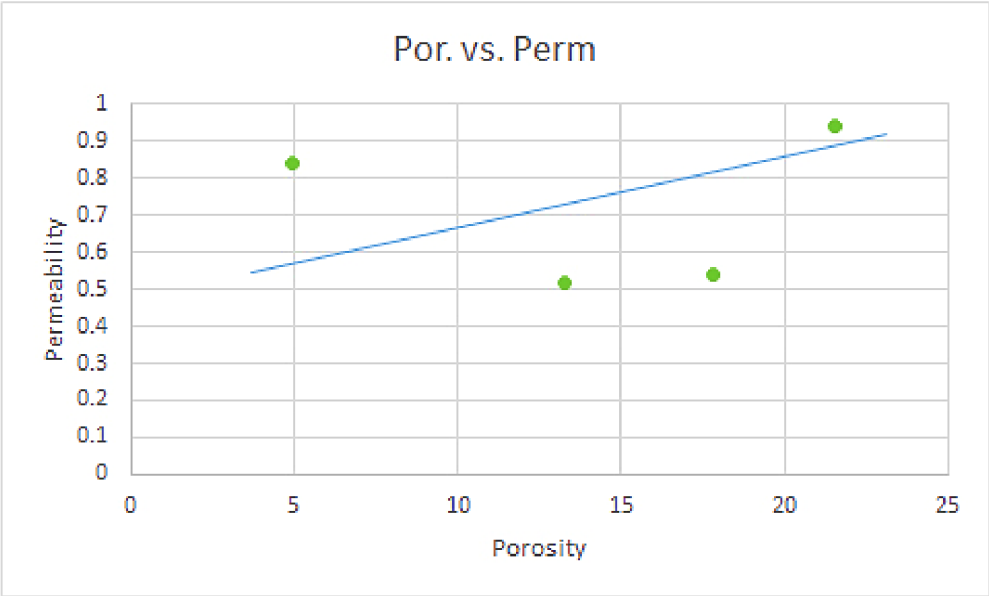
Figure 15 Relationship between porosity (%) and permeability (mD) for outcrop section

5.7. Thin section

Samples results are from Khurmala Formation in Shaqlawa section in Kurdistan region of Iraq which blue spots obtained to be porosity which the porosity of the thin sections measured by a program (ImageJ) the thin sections and the results are shown in (figs.15,16,17,18,19,20,21): -

Figure 16 thin section sample for layer 2 in the Khurmala formation in Shaqlawa the porosity was 5 %

Figure 17 thin section sample for layer 7 in the Khurmala formation in Shaqlawa the porosity was 10 %

Figure 18 thin section sample for layer 7A in the Khurmala formation in Shaqlawa the porosity was 5 %

Figure 19 thin section sample for layer 7B in the Khurmala formation in Shaqlawa the porosity was 20 %
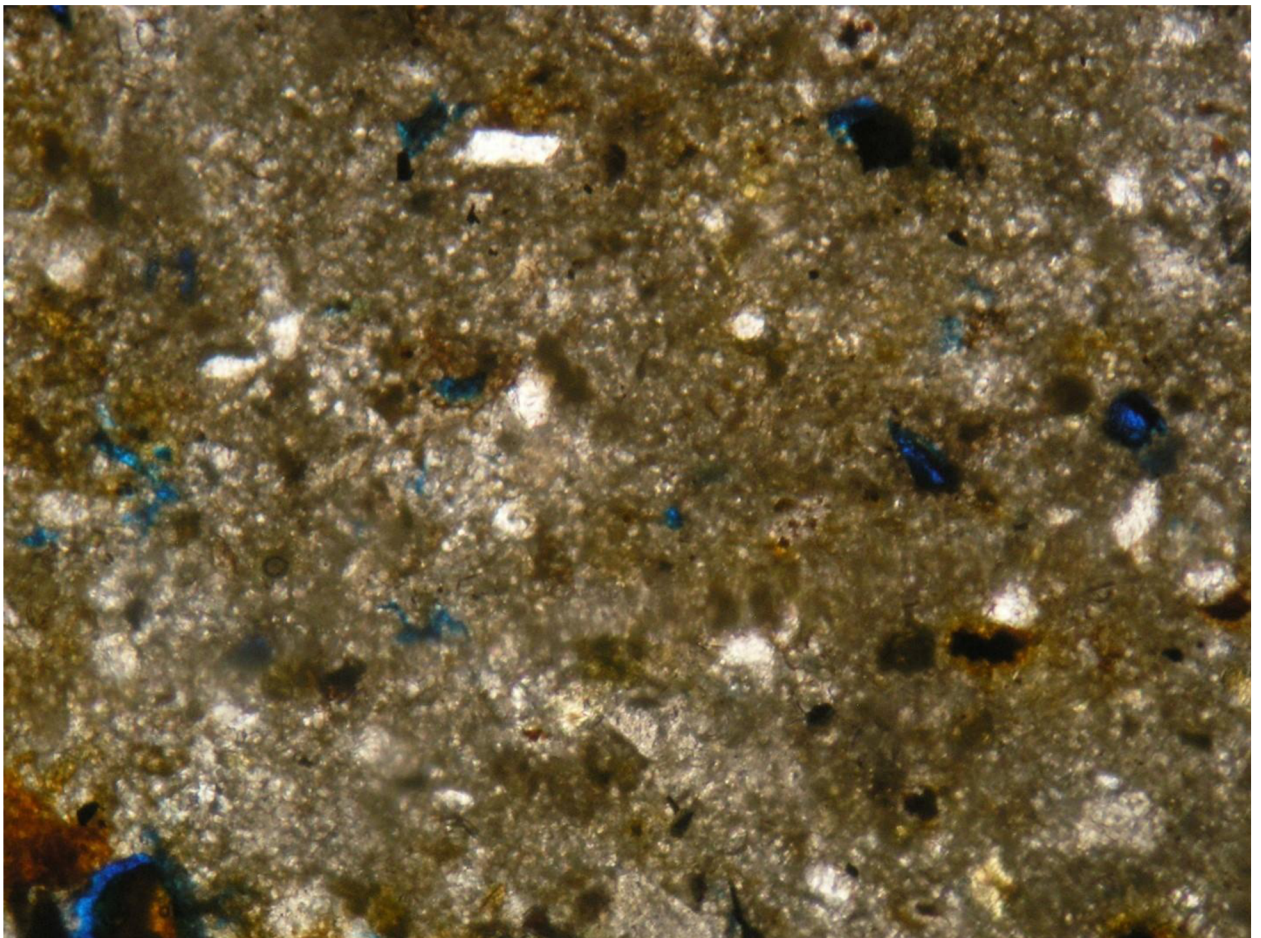
Figure 20 thin section sample for layer 5 in the Khurmala formation in Shaqlawa the porosity was 15 %
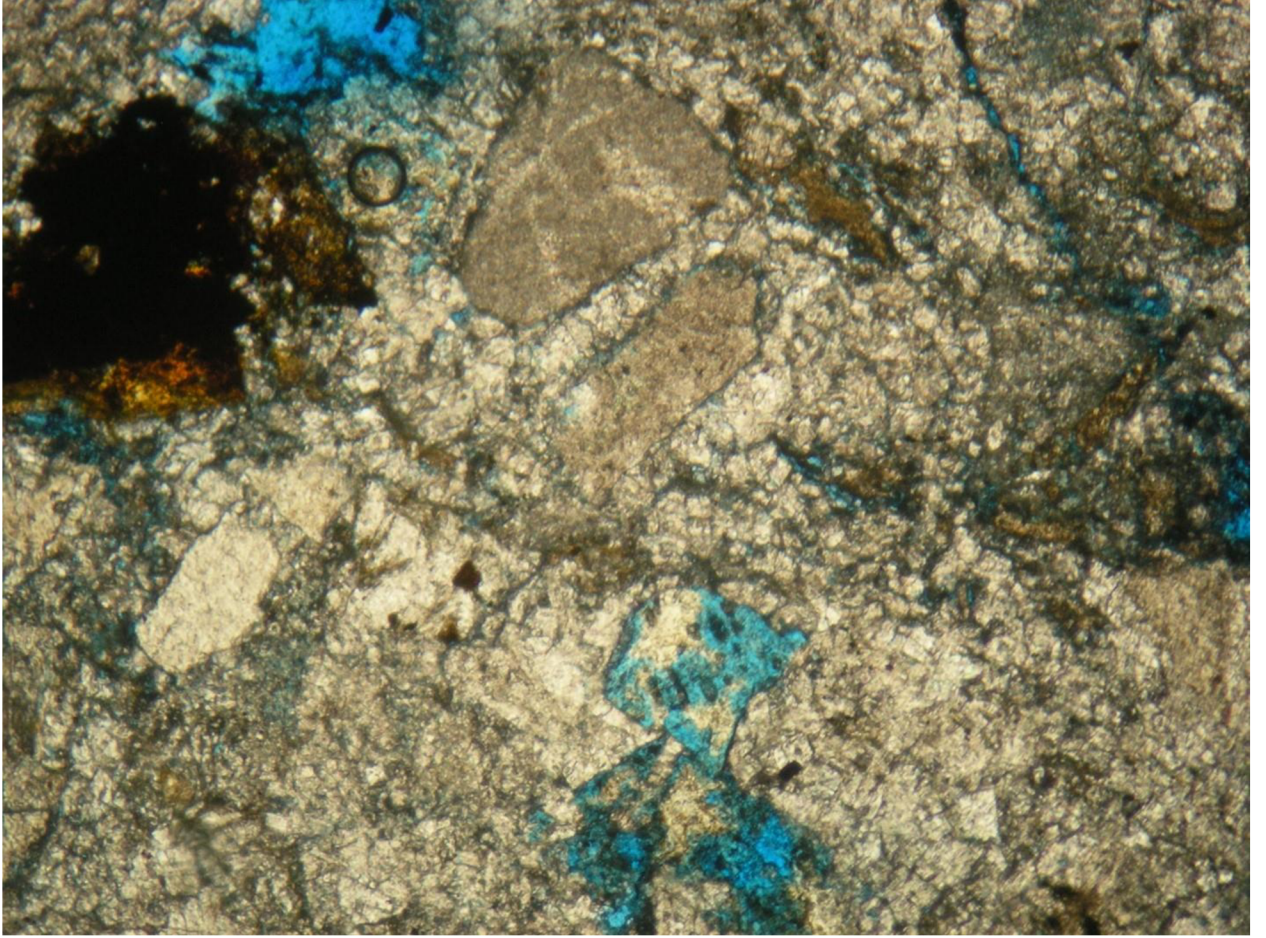
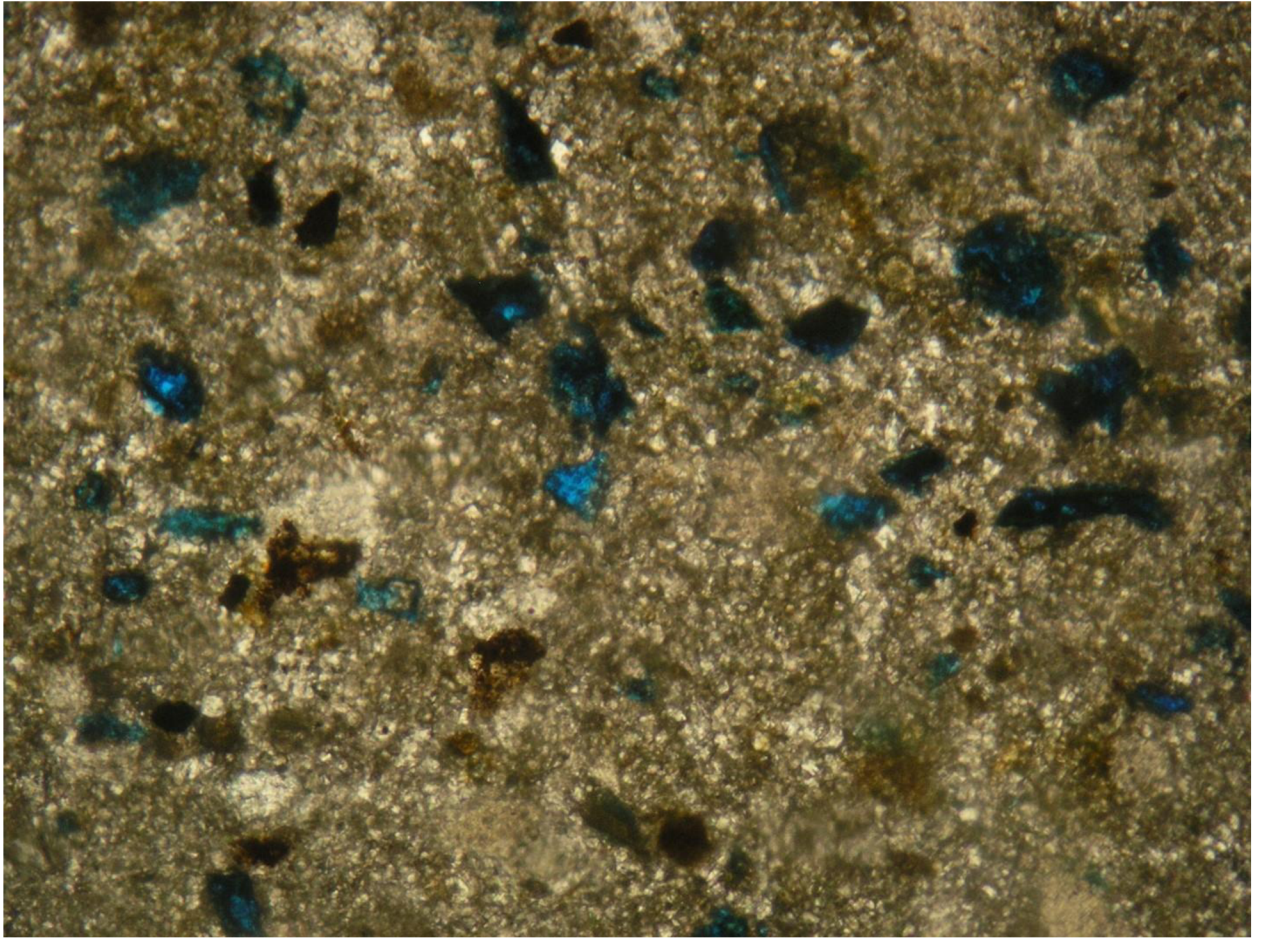Figure 21 thin section sample for layer 8 in the Khurmala formation in Shaqlawa the porosity was 10 %
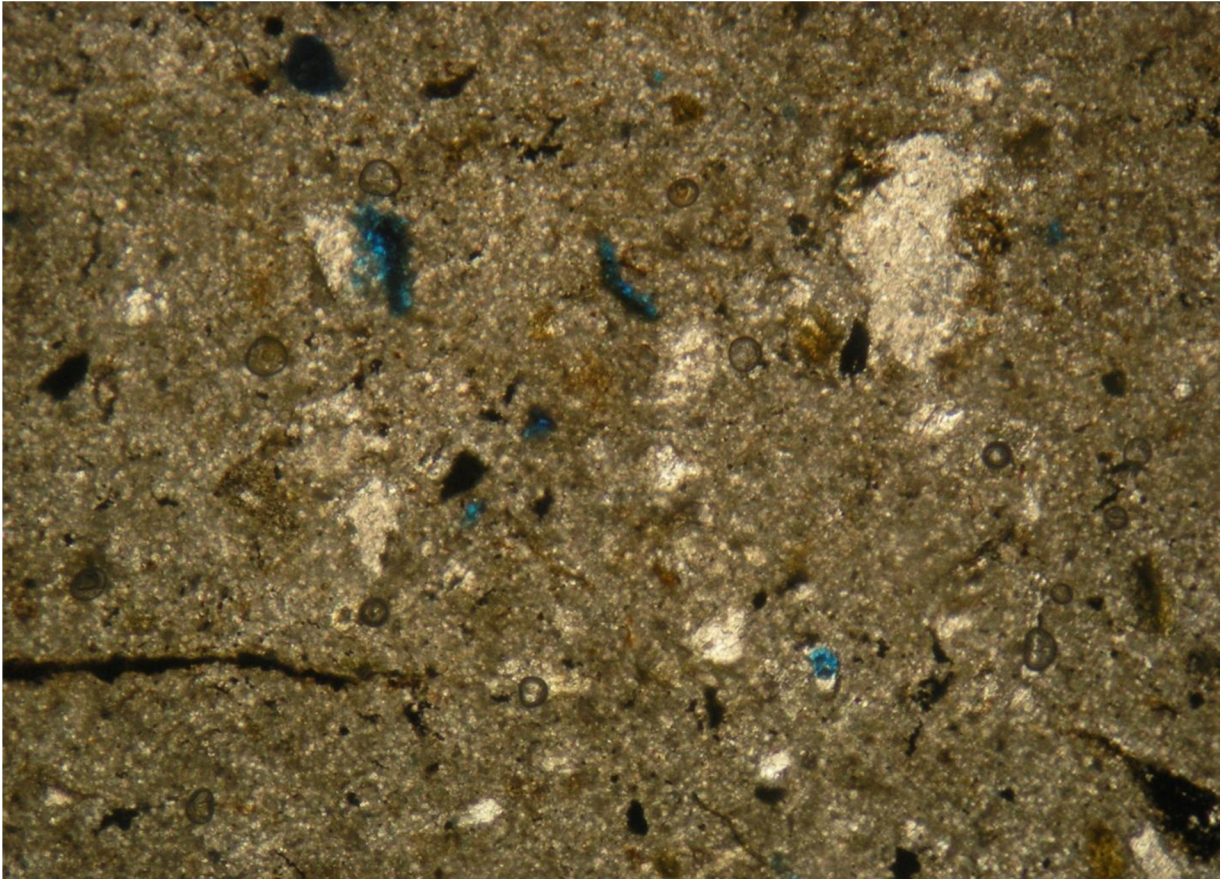
Figure 22 thin section sample for layer 16 in the khurmala formation in Shaqlawa the porosity was 3 %
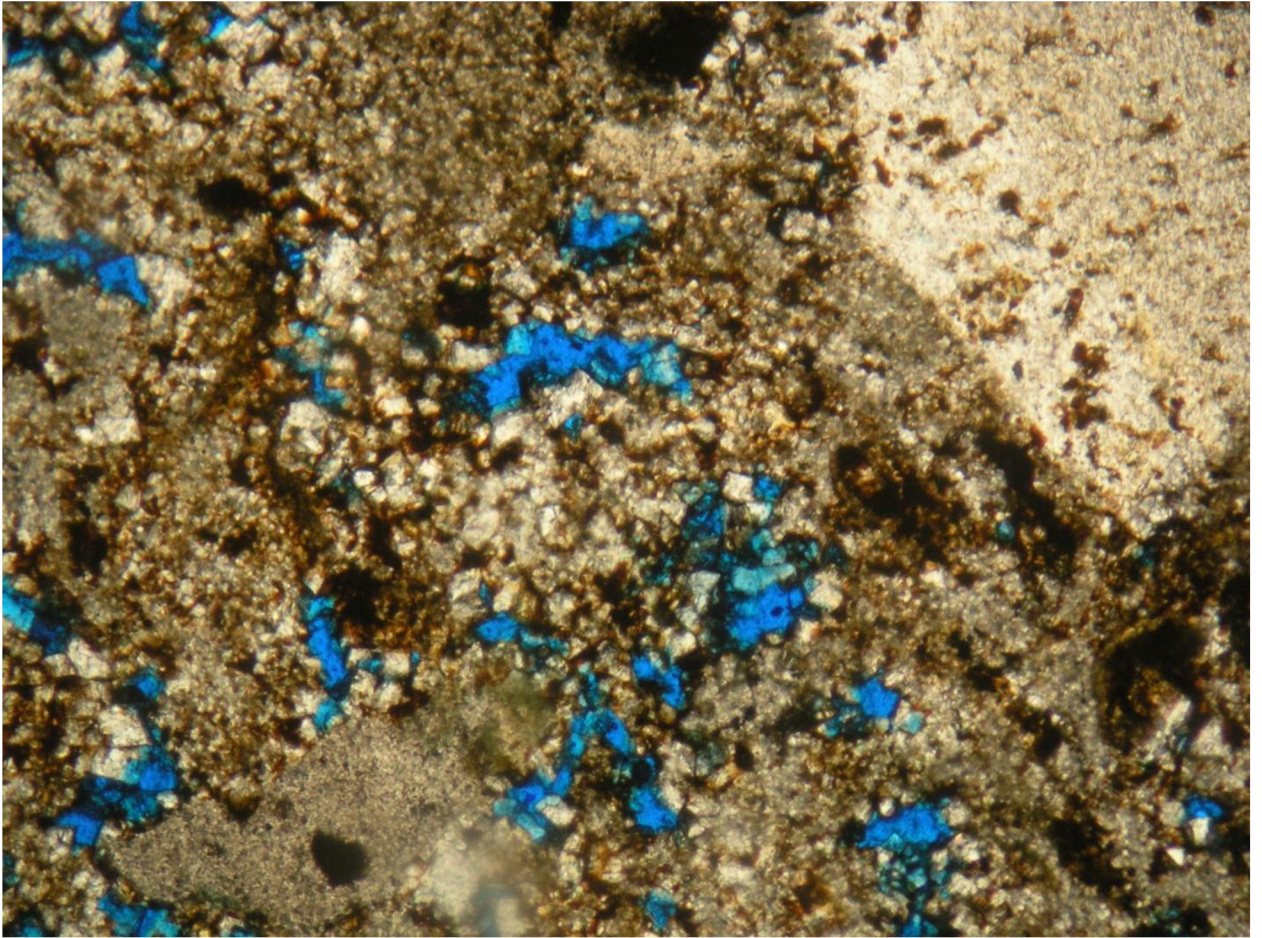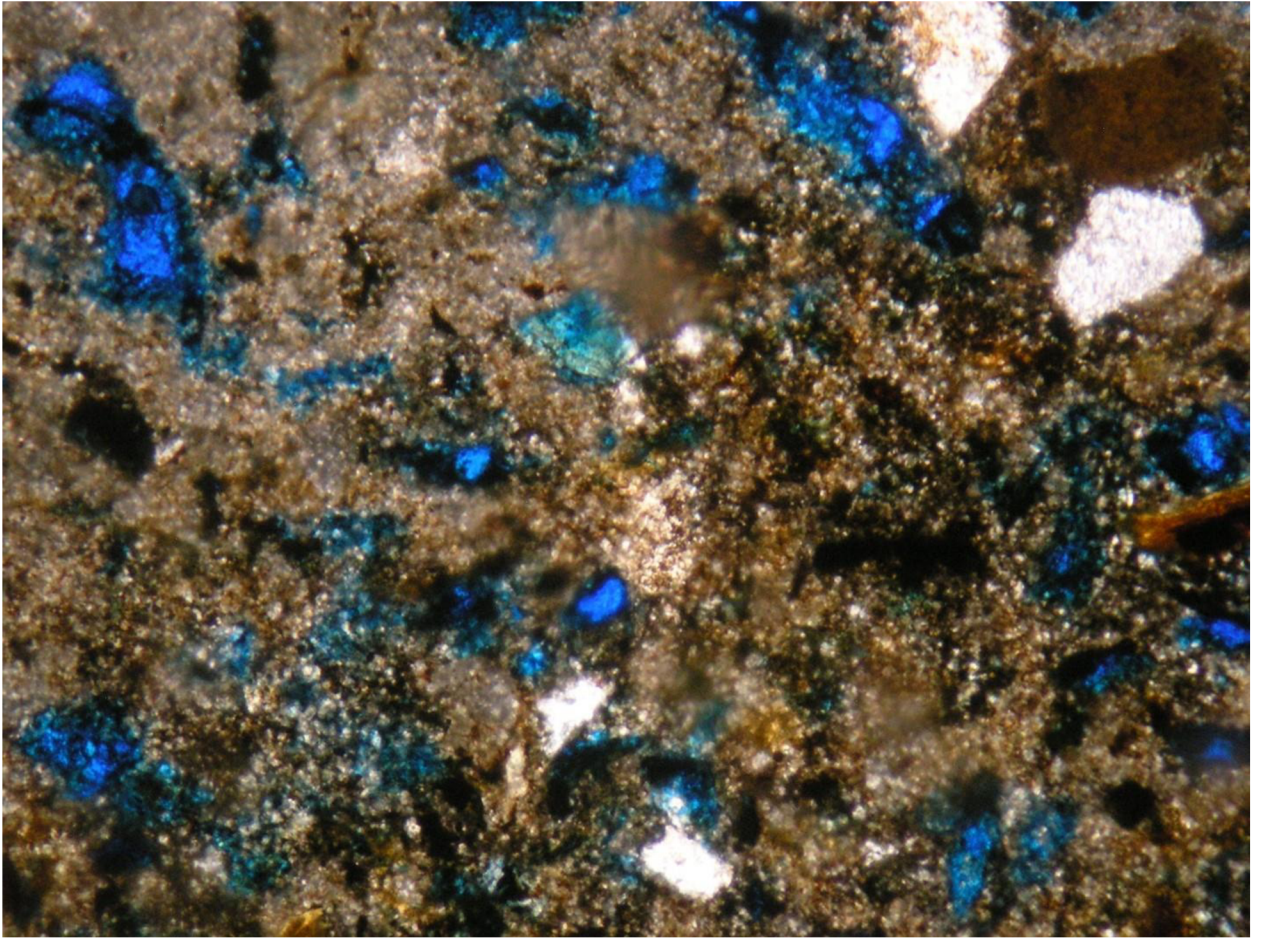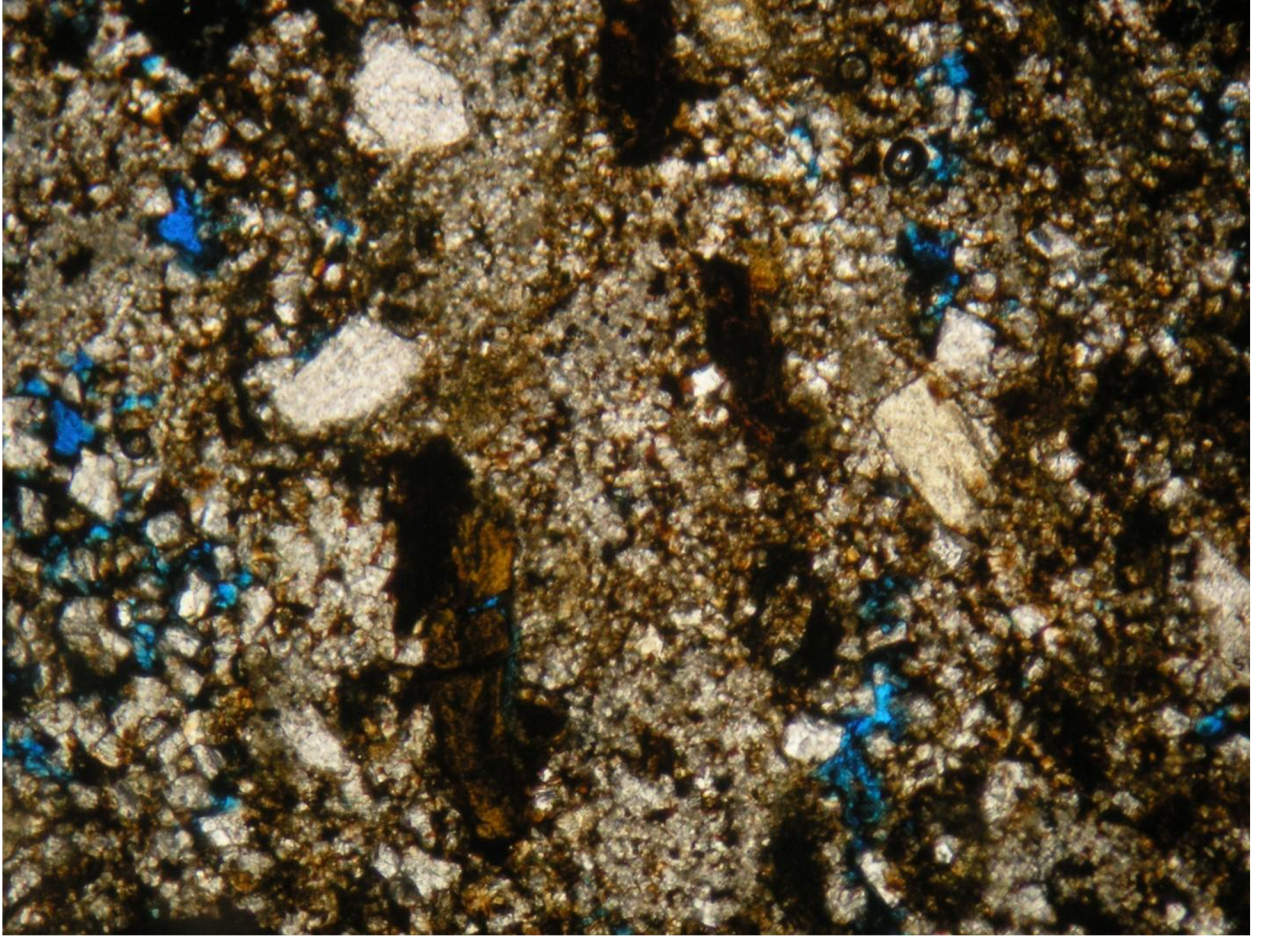
Chapter 5: Discussions

5. Pore pressure and fluid contact

5.1. Analysis of reservoir fluids

The volume of any given liquid in the pore space is known as its saturation, and the saturation is a percentage or fraction of the overall capacity to store liquids (porosity), which in essence holds any fluid. The determination of saturation and hydrocarbon movability reveals which permeable zones may be of interest (Pickett, 1966).

5.1.1 Water saturation (Sw)

Water saturation Is the volume of pores which the formation water has been filled in a rock.

Decimal fractions or percentages are used to describe water saturation (Asquith and Krygowski 2004).

$$Sw = \left(\frac{a}{\emptyset^m} * \frac{Rw}{Rt}\right)^{\frac{1}{n}} \dots\dots\dots\dots\dots (9)$$

The Archie's (1942) formula is used to compute Sw of a reservoir's uninvaded zone:

$$Sxo = \left(\frac{a}{\emptyset^m} * \frac{Rmf}{Rxo}\right)^{\frac{1}{n}} \dots\dots\dots\dots\dots\dots (10)$$

The moveable hydrocarbon can be identified by water saturation of the flushed zone (Sxo). If Sxo is larger than Sw, hydrocarbons in the flush zone are most likely to be moved or flushed out of the area close to the bore hole by invading drilling fluids (Asquith, and Krygowski, 2004). The Sxo values in this study are more than Sw, indicating that the rocks under examination have a high moveable hydrocarbon content.

5.1.2 Water volume in bulk (Bvw)

Before the hydrocarbon migrated to the reservoir rocks and was recognized as connate water, the entire amount of bulk water that was preserved in sediments throughout deposition and lithification is referred to as bulk water volume (Tiab and Donaldson, 1996). The result of the saturation of the formation water and the effective porosity of the water is a large bulk volume of water (BVW) in the uninvaded zone., while the bulk volume of water (BV_{SXO}) The product of the formation water saturation (Sxo) and the effective porosity shall be given to the flushed zone. (Spain, 1992).

The mobile hydrocarbon is characterised by the area between BVWsxo and BVW, however the residual hydrocarbon is signified by the area between BVWsxo and φe

5.1.3 Saturation of hydrocarbons (Shc)

The following relationship may be used to infer the hydrocarbon saturation from the water saturation:

Hydrocarbon saturation is often classified as a non-exploitable or residual hydrocarbon (Shr), or an exploitable or moveable hydrocarbon (Shm), as shown below:

$$Shc = 1 - Sw \dots \dots \dots \dots \dots .(11)$$

$$Shc = Shr + Shm \dots \dots \dots \dots \dots .(12)$$

On the computer processing interpretation (Fig. 23), In the lower part of the formation, due to the high porosity, mobile hydrocarbons can be observed in the subsurface section.
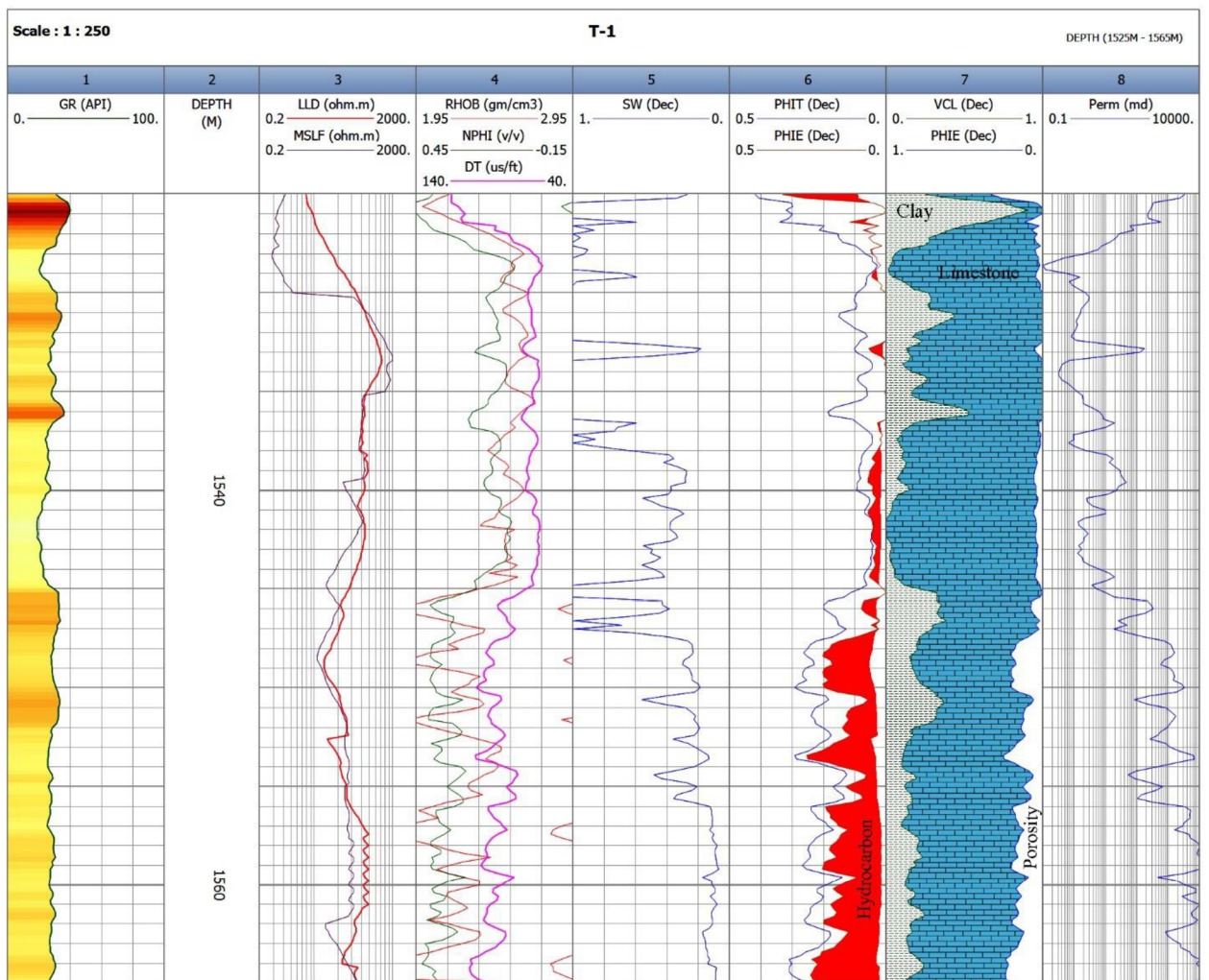
Figure 23 Computer processing interpretation (CPI) for the Khurmala Formation in Tawke Oil Field, saturation and net pay have been shown in depth interval 1540-1565m

5.2 Pore pressure

The force exerted by the fluid inside the formation's pores is sometimes referred to as pore pressure. Overpressure occurs when the pore pressure is greater than the hydrostatic pressure. For safe well design, effective reservoir modelling, and cost-effective drilling, knowledge of this pressure is crucial. The major goal of this work is to use well log data from one of the oil fields in the north of Iraq to estimate the formation pore pressure as a trustworthy mud weight pressure.

It can be classified as normal or abnormal depending on the size of the pore pressure. Normal pore pressure is the state in which the pore pressure equals the hydrostatic pressure. The permeable sediments link formations under normal pressure to a free surface. Pore pressure that is abnormally high (overpressure) or low (under pressure) compared to hydrostatic pressure is addressed (Swarbrick et al., 1998).

5.2.1 Pore pressure estimation methods

Various approaches to pore pressure estimations have been put forth. The first investigation of pore pressure estimation using shale parameters derived from borehole data was carried out (Hottman and Johnson in 1965). This method was used to interpret any departure from the typical trend line in the observed parameters as an indication of anomalous pore pressure. Later, other researchers have successfully predicted pore pressure using well log data like as resistivity, sonic transit time, porosity, and others. Most of these investigations are predicated on the concept that any changes in a region with normal pore pressure cause changes in petrophysical parameters such as compaction, porosity, and fluid motion.

Therefore, the interpretation and quantitative evaluation of pore pressure can be based on all observable characteristics which can show these changes in some way (Azadpour et al., 2015). Pore pressure estimation methods like as Eaton's, Bowers', and Holbrook's are widely utilized in the oil business.

Pore pressure is frequently calculated using Terzaghi's relationship and well log analysis. The vertical effective stresses and pore pressures of this relationship affect the overburden load. Terzaghi (1943) assumed the following relationship:

$$S = P + \sigma \dots\dots\dots\dots (13)$$

Where, S is the overburden pressure (the related weights of formation solid and fluid); σ is the vertical effective stress (the grain-to-grain connection stress) and P correspond to the pore pressure.

The Eaton Approach, which views compaction disequilibrium as a key process in the development of overpressures, is one of the most commonly used techniques for predicting pore pressure. Using well log data, Eaton (1975) established an empirical equation to calculate the pore pressure. This approach assumes that, as Terzaghi's equation illustrates, pore pressure and vertical effective stress sustain overburden pressure. Eaton provided the empirical equation shown below for pore pressure prediction using sonic transit time in accordance with above (Equi 14):

$$Gp = Go - (Go - Gn) \left(\frac{\Delta tn}{\Delta to}\right)^x \dots\dots\dots\dots (14)$$

where, Gp, Go, and Gn are, the overburden pressure gradient, and the hydrostatic pressure gradient respectively; Δto stands for the measured sonic transit time by well logging and Δtn is the normal sonic transit time in shale obtained from normal trend line; x represents the exponent constant.

Bowers' approach is based on effective stress to determine pore pressure. The essential step in this approach is to compute effective stress from velocity and then apply Terzaghi's equation to determine pore pressure. The major processes of overpressure creation in this approach are compaction disequilibrium and unloading owing to fluid expansion. Bowers (1995) suggested the following experimentally proven method for calculating effective stress under compaction disequilibrium conditions:

$$V = Vo + A\,\sigma^B \dots\dots\dots\dots\dots\dots (15)$$

where, V is the velocity in the given depth and $V0$ lasts for the velocity in the surface (normally 1500 m/sec); σ represents the vertical effective stress; A and B parameters are taken from calibrating regional

A pore pressure estimates techniques for naturally reservoirs fractured was also make known by Holbrook (1999). Holbrook's approach does not need the establishment of some trend lines because it is based on the correlation between effective stress, mineralogy, and porosity in granular sedimentary rocks. Holbrook had been able to accurately predict pore pressure in intervals of limestone, shaly limestone, and sandstones in the North Sea. (Holbrook, 1999). The following equation is used in Holbrook's approach to determine the rock's effective stress:

$$\sigma = \sigma\,max\ x\ (1\text{-}\varphi)^{B} \ldots\ldots\ldots\ldots\ldots. \ (16)$$

where, σmax is the maximum effective stress required to reduce the mineral porosity to zero and φ is porosity from well logs; β stands for the compaction strain-hardening coefficient for the type of minerals.

Weakley's approach

Because of the geological complexity of carbonate settings, determining pore pressure from log characteristics has always been difficult. As opposed to shales, they do not compress evenly with depth. Indeed, applying conventional pore pressure prediction methods to carbonate rocks does not necessarily result in an accurate forecast. By using sonic velocity patterns, Weakley (1990) developing a method for measuring the pressure of the pore formation in carbonates. For each part of that formation, he applied the trends in sonic wave velocity based on an Eaton theory. These formation portions were identified as the lithology changing index from well log replies by joining the final value of interval velocity trend from an earlier lithology section with the first value in the next, a smooth continuous ultrasonic velocity log was created that used Eaton's approach to estimate pore pressure. The detection of normal compaction trend line, normal compaction trend (NCT), and proper exponent constant x, which was initially 3 in Eaton's research's and needs adjustment for using in tight unconventional reservoirs, are the most effective parameters in Eaton's approach (Contreras et al., 2011).

For the determination of a normal compaction trend line, it is necessary to use traditionally valid well log data. Any deviation from a normal trend line constitutes an indication of abnormal pressure. For the exponent constant x, an equation of Eaton's is given as follows:

$$X = \frac{Log\left(\frac{Go-Gp}{Go-Gn}\right)}{\log\left(\frac{\Delta Tn}{\Delta To}\right)} \quad \dots\dots\dots\dots (17)$$

The gradient of normal hydrostatic pressure (Gn), according to studies conducted in the Middle East, is 10.5 kpa/m (Atashbari et al., 2015).

In Northern Iraq, the studied oil field is located. The formation of the reservoirs is composed of shale, dolomite, and limestone. Khurmala is part of the study formation. It is a hard limestone formation of the Paleocene-Eocene, the porosity in the top region is relatively weaker compared to the bottom.

To determine pore pressure in this study, the data from one of the wells is used together with other petrophysical logs such as transient time, gamma rays, and density measurements along with mud weight pressures. When there is evident noise, such as hole washouts or cycle skips on the sonic log, bad data is repaired. Additionally, software corrects environmental impacts such wellbore caving, mud salinity, mud pressure, and mud cake. This study's objective is to assess pore pressure in carbonate reservoirs using Weakley's methodology and compare the findings to pore pressure predictions made using the standard Eaton's method.
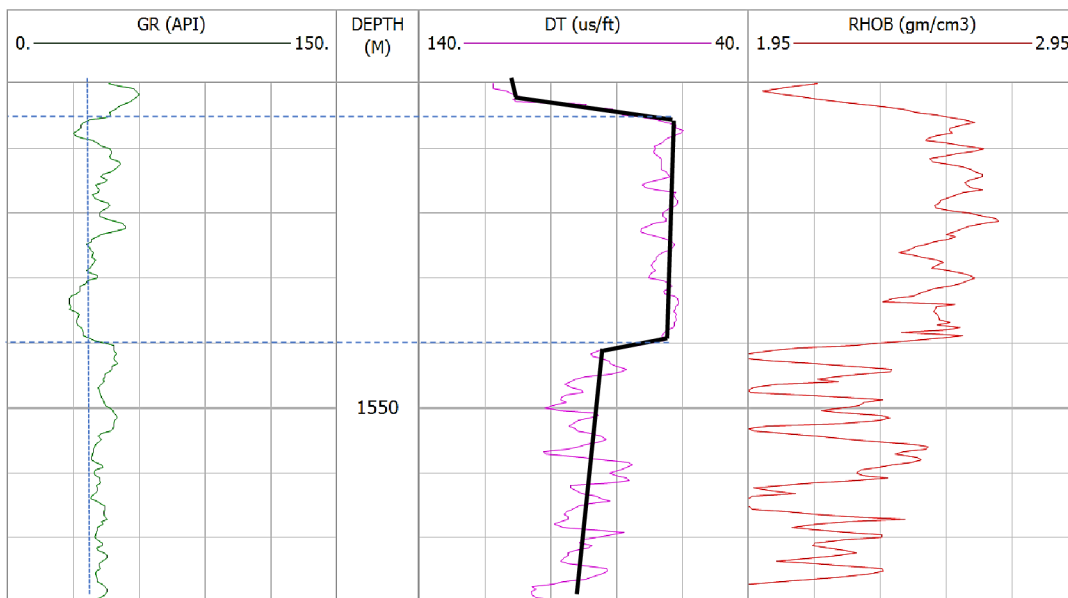

Figure 24 Lithology separations based on changes in petrophysical properties (GR, DT, and RHOB); trend lines are detected based on gamma ray peaks trend to the right for each lithology section.

41

Finding the lithology tops is the first stage in Weakley's method. Gamma ray, density, and sound logs are used to separate various lithologies in this process. Lithology tops are selected at the locations where the overall trend in the gamma-ray, density, or sonic logs changes.

The gamma ray peaks within lithological sections were examined, and the results revealed a tendency toward the right in the shale direction. It is possible to identify the sonic velocities, which correlate to the gamma ray peaks. As seen in (Fig 24), trend lines have been created in relation to these sonic velocity peaks. In Weakley's method, the final interval velocity value of a lithological section is merged with the first values from each other in order to shift sonic tendency lines during transitional lithology. As shown in (Fig25) (a & b), this recalibrates the outcomes in a continuous relative interval sonic transient time (DT):

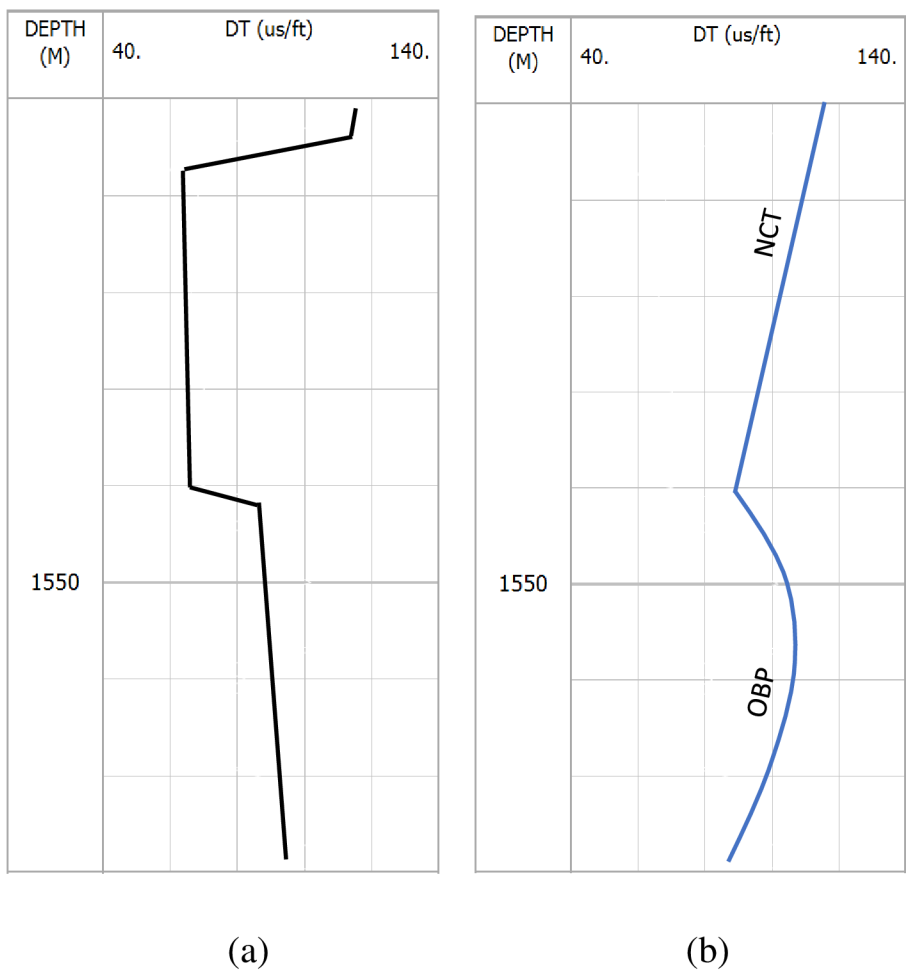(a)   (b)

Figure 25 (a&b) (Sonic transient time calibration with Weakley's approach trend lines within lithologies a and b) DT log and recalibrated DT trend lines.

As shown in the (fig.26) the selected interval has no change in normal compaction trend while the other pressures have been changed, overburden pressure which represented by blue colour depends on the total compressibility of the rock and is almost constant in the formation, Despite the fact that the measured hydrostatic pressure has been constant for a predetermined amount of time, the major cause of this rise (after depth 1550m) is an increase in density or the entry of additional fluids; The fluids in the voids are the primary cause of the considerable increases and decreases in pore pressure, which is in addition to the formation pressure, which observes a variation in the special value as a consequence of the different types of rocks from one layer to the others.
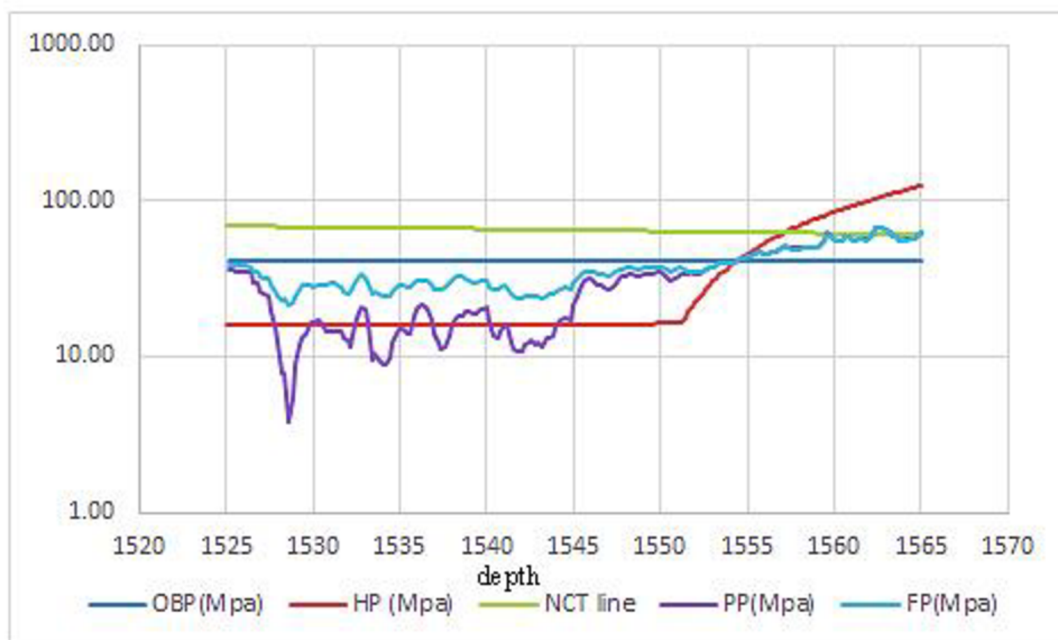
Figure 26 drawing depth vs. all parameters related to pressures (overburden (OBP), hydrostatic (HP), pore (PP)and formation pressure (FP) respectively)

Discussion the relation between porosity, water saturation, and pore pressure

The research region is located mostly in the Tawke oilfield and outcrop Shaqlawa district, between latitudes 36N and 44E. To better understand the hydrocarbon potentialities of the Khurmala Formation using tawke-1 well, it is being studied in combination with underground geology investigations, borehole reviews and petrophysical laboratory data.

Well logs of several forms for determining petrophysical parameters (shale content, porosity, and fluid saturation). The porosities were also calculated using the available acoustic, density, and neutron records. Based on the results of the flow line, background gases, mud density, and wireline logs, the outcomes were chosen for estimating the pore pressure for the Khurmala Formation. There found a correlation between pore pressure levels and hydrocarbon saturation.

Evaluation of formation pressures is a part of the procedure for developing wells and evaluating formations. In order to optimize the mud density and ensure an adequate level of imbalance in a well drilled with safety and minimal cost, it is essential that we know the pressure from the pore as well as fractures.

The Khurmala Formation in selected areas is composed of carbonate and shale, the characteristics of such reservoir are summarized as follows: the reservoir average parameter values were as value the shale content from 0.2%, effective porosity from 3 to 14%, while the water saturation from 20 to 28%, finally the hydrocarbon saturation average value 80%. The average of calculated formation pore pressure ranges from 0.4 ppg to 9 ppg. The studied well can be divided into two zones of pore pressure designated as normal pressure zone and abnormal pressure zone in this closed system reversal pressure has been developed due to the possibility of gas dissolved in water in the lower part, which has been a result of increasing pressure caused by sediment subsidence. Finally, the Khurmala Formation in the Tawke field is regarded as a promising reservoir with high pore pressure values and strong hydrocarbon potentialities.

Chapter 6: Conclusion

- According to the calculated shale from gamma-ray log, the Kurmala Formation can be considered as shaly formation.
- The neutron-density cross-plot showed that the Khurmala reservoir consists mainly of limestone and dolomitic limestone.
- based on porosity model, fair and good porosity and permeability are present in the lower part of the Early Tertiary formation in this well and the porosity types are secondary porosity. The same result can be seen clearly in the outcrop section
- The results of the study of carbonate formation and the claim that the formation of the pore pressure occurs after 1550 m are provided by the prediction and modelling of the pore pressure based on the sonic well log.

References

Adam, A., Swennen, R., Abdulghania, W., Abdlmutalib, A., Hariria, M. and Abdulraheem, A., 2018. Reservoir heterogeneity and quality of Khuff carbonates in outcrops of central Saudi Arabia. Marine and Petroleum Geology, 89, pp.721-751.

Alavi M 1994. Tectonics of the Zagros orogenic belt of Iran: new data and interpretations. Tectonophysics 229:211–238.

Alavi M 2004. Regional stratigraphy of the Zagros fold-thrust belt of Iran and its proforeland evolution. Am J Sci 304:1–20.

Al-Banna N. Y. Al-Mutwali M. M. Al-Ghrear J. S. 2006. Facies Analysis and Depositional Environment of Khurmala Formation in Bekhair Anticline –Dohuk Area, North Iraq, Iraqi Jour. Earth Sci., Vol.6, No.2, pp.13-22,

Al-Lihaibi S. F. 2012 Diagenesis of Khurmala Formation in Dokan Area, North Eastern Iraq, Iraqi National Journal of Earth Science, 2012, Volume 12, Issue 3, Pages 17-34

Al-Qayim B. Barzani A. T. 2021 Facies and stratigraphic associations of Sinjar and Khurmala Formation, Dohuk Area, Kurdistan Region, Iraq, Geography, Environmental Science, Geology

Al-Qayim, B.A. and Othman, D.H., 2010. Lithofacies association, dolomitization, and potentiality of the pila spi formation, taq taq oil field, Kurdistan region, NE Iraq. Iraqi Bulletin of Geology and Mining, 6(2), pp.95-114.

Al-Qayim, B. and Rashid, F., 2012. Reservoir characteristics of the albian upper qamchuqa formation carbonates, Taq Taq oilfield, Kurdistan, Iraq. Journal of Petroleum Geology, 35, pp.317-341.

AQRAWI, A.A.M., GOFF, J.C., HORBURY, A.D. and SADOONI, F.N., 2010. The

Petroleum Geology of Iraq: Scientific Press.

Asaad, I. S., Balaky, S.M., 2018. Microfacies analysis and depositional environment of Khurmala Formation (Paleocene-Lower Eocene), in the Zenta Village, Aqra District, Kurdistan Region, Iraq. Iraqi Bulletin of Geology and Mining, 14(2), 1-15.

Asaad I. Sh., Al-Haj M. A. and Malak Z.A. 2022 Depositional Setting of Khurmala Formation (Paleocene-Early Eocene) in Nerwa section, Berat Anticline, Kurdistan Region, Northern Iraq, Iraqi Geological Journal 2022, 55 (1F), 20-39

ASQUITH, G.B. and GIBSON, C. 1982. Basic well log analysis. Second edition AAPG, Tulsa, Oklahoma.

ASQUITH, G. and KRYGOWSKI, D. 2004. "Basic Well Log Analysis". Second edition.

Atashbari, V. and Tingay, M., Pore Pressure Prediction in Carbonate Reservoirs, in SPE Latin America and Caribbean Petroleum Engineering Conference, 2012.

Azadpour, M., Shad Manaman, N., Kadkhodaie-Ilkhchi, A., and Sedghipour, M.R., Pore Pressure Prediction and Modeling using Well-logging Data in One of the Gas Fields in South of Iran, Journal of Petroleum Science and Engineering, Vol. 128, p. 15-23, 2015.

BELLEN, R.C., DUNNINGTON, H.V., WETZEL, R. and MORTON, D. (1959)

Lexique Stratigraphic International. Asie, Fasc. 10a, Iraq, Paris p 333.

Bhuyan, K. and Passey, Q.R., 1994. Clay Estimation from Gamma Ray and Neutron-density Porosity Logs. SPWLA, 35thAnnual Logging Symposium, Tulsa.

Bowers, G., Pore Pressure Estimation from Velocity Data: Accounting for Overpressure Mechanisms Besides Undercompaction, SPE Drilling & Completion, Vol. 10, No. 2, p.89-95, 1995.

Contreras, OM, Tutuncu, AN., Aguilera, RM., and Hareland, GM., a Case Study for Pore Pressure Prediction in an Abnormally Sub-pressured Western Canada Sedimentary Basin, in 45th US Rock Mechanics/Geomechanics Symposium, 2011.

Doski J. 2019 Tectonic interpretation of the Raniya earthquake, Kurdistan, northern Iraq, J Seismol 23:303–318.

Eaton, B., the Equation for Geopressure Prediction from Well Logs, in Fall Meeting of the Society of Petroleum Engineers of AIME, 1975.

Fouad SFA (2014) Western Zagros fold–thrust belt, part II: the high folded zone. Iraq Bull Geol Mini Special Issue 6:53–71.

Ghafur, A.A. and Hasan, D.A., 2017. Petrophysical properties of the upper qamchuqa carbonate reservoir through well log evaluation in the Khabbaz oilfield. Journal of Science and Engineering, 1(1), pp.72-88.

Holbrook, P., A Simple Closed Form Force Balanced Solution for Pore Pressure, Overburden and the Principle Stresses, Earth Marine and Petroleum Geology, Vol. 16, p.303-319, 1999.

Hollis, C., 2011. Diagenetic on controls reservoir properties of carbonate successions within the Albian turonian of the Arabian plate. Petroleum Geoscience, 17, pp.223-241.

Hollis, C., Lawrence, D.A., Perière, M.D., Al Darmaki, F., 2017. Controls on porosity preservation within a Jurassic oolitic reservoir complex, UAE. Marine and Petroleum Geology, 88, pp.888-906.

Hottmann, CE. and Johnson, RK., Estimation of Formation Pressures from Log-derived Shale Properties, Journal of Petroleum Technology, Vol. 17, No. 06, p.717-722, 1965.

Hussein, D., Lawrence, J., Rashid, F., Glover, P. and Lorinczi, P., 2018. Developing Pore Size Distribution Models in Heterogeneous Carbonates Using Especially Nuclear Magnetic Resonance. In: Engineering in Chalk: Proceedings of the Chalk 2018 Conference. ICE Publishing, London. pp.529-534.

Jafarian, A., Fallah-Bagtash, R., Mattern, F. and Heubeck, C., 2017. Reservoir quality along a homoclinal carbonate ramp deposit: The permian upper Dalan formation, South pars field, Persian Gulf Basin. Marine and Petroleum Geology, 88, pp.587-604.

JASSIM, S.Z. and GOFF, J.C. 2006. Geology of Iraq. Czech Republic: Dolin,

Prague and Moravian Museum, Brno.

Krygowski, D.A., 2003. Guide to Petrophysical Interpretation. Wyoming University, Austin Texas USA. p.147.

Mukherjee S, Kumar N 2018. A first-order model for temperature rise for uniform and differential compression of sediments in basins. Int J Earth Sci 107:2999– 3004

Mzuri R. T and Omar A. 2016 Extraction and Analysis of Tectonic Lineaments using Geoinformatic Techniques, in Tawke Oil Field, Duhok area, Iraqi Kurdistan Region journal of zankoy slemani conference

Pickett, G.R. 1966. A Review of Current Technique for Determination of water saturation from logs. SPE 1446 p.

Rashid, F., Glover, P.W.J., Lorinczi, P., Hussein, D. and Lawrence, J., 2017. Microstructural controls on reservoir quality in tight oil carbonate reservoir rocks. Journal of Petroleum Science and Engineering, 156, pp.814-826.

Rashid, F., Hussein, D., Lawrence, J.A. and Khanaqa, P., 2020. Characterization and impact on reservoir quality of fractures in the cretaceous qamchuqa formation, Zagros folded belt. Marine and Petroleum Geology, 113, pp.104-117.

Rider, M.H. and Kenedy, M., 2011. The Geological Interpretation of Well Logs. Rider-French Consulting Ltd., Sutherland. p.280

Ryder Scott Company, 2011. Estimated Unrisked Discovered and Undiscovered Total Petroleum Initially in Place Attributable to Certaininterests in the Shaikan License Block, Kurdistan, Iraq. Report Prepared for Gulf Keystone Petroleum Ltd., Iraq.

Schlumberger 1974. Log interpretation, vol. II—applications. Schlumberger, New York

Schlumberger, 1997. Log Interpretation/Charts. Schlumberger Wireline and Testing, Houston, USA.

Schlumberger, 2012. Definition of porosity: How porosity is measured. Oil Field Review Autumn, 24(3), pp.63-64.

SELLEY, R.C. (1985-1998) Elements of petroleum geology. San Diego – London,

UK: second edition, Academic press.

Sherwani, G.H. and Zangana, H.A. 2017. Reservoir characterization of early jurassic formations in selected wells in the duhok governorate, Iraqi Kurdistan region. Journal of Science and Engineering, 1(1), pp.11-18.

SPAIN, D.R. 1992. Petrophysical Evaluation of a slope Fan / Basinfoor Fan

Complex, Cherry Canyon Formation. AAPG Bulletin. 76(6). p.805-827.

Swarbrick, B. E. and Osborne, M. J., Mechanisms that Generate Abnormal Pressures, an Overview, Memoirs-American Association of Petroleum Geologists, p. 13-34, 1998.

Terzaghi, K., Theoretical Soil Mechanics, 1943.

TIAB, D. and DONALDSON, E.C. (1996) Petrophysics, Theory and Practice of Measuring Reservoir Rock and Fluid Transport Properties. Huston, Texsas.

Weakley, R. R., Determination of Formation Pore Pressures in Carbonate Environments from Sonic Logs, in Annual Technical Meeting, Petroleum Society of Canada, 1990.

Wiley, R. and Pachett, J.G., 1990. CNL (Compensated Neutron Log) Neutron Porosity Modeling, a Step Forward. SPWLA 30th Annual Logging Symposium.

ZebariM (2013) Geometry and evolution of fold structures within the high folded zone: Zagros fold-thrust belt, Kurdistan region-Iraq. MSc Thesis, University of Nebraska-Lincoln, p.91